Application of TAPM in Swedish west coast:

Modeling results and their validation during 1999-2000

Deliang Chen[1,2], Tijian Wang[1,2], Marie-Haeger Eugensson[1]

Christine Achberger[2], Katarina Borne[2]

[1]IVL Swedish Environmental Research Ltd

[2]Earth Sciences Centre, Gothenburg University

Content

Abstract

TAPM, The Air Pollution Model, was developed by Australian CSIRO Atmospheric Research Division. It is a 3-D meteorological and chemical model for air pollution studies. TAPM has been applied by IVL since 1999. To our knowledge TAPM has not yet been tested against observation in Sweden before. This report summarizes an extensive simulation during 1999-2000 with Swedish west coast in focus. First it gives a brief description of TAPM. Then the details of the simulation including setup of the model and choices made in modeling were explained. Three nesting were used to come down to the finest resolution of 1 km. The modeled results in terms of the surface air temperature and wind, as well as vertical profiles of wind, have been compared with available observations to examine TAPM's performance for local meteorology that is often central to air pollution modeling in coastal area. The NCDC surface meteorological data and sound radar (SOD[illegible]) data collected by Älvborgsluftförbundet were used for the comparison. Investigations have shown that the model performs well in simulating air temperature and wind, which are the two most important fields to drive air pollution modeling. Also, TAPM was confirmed to have strong ability in simulating thermally driven meso-scale systems, such as sea-land breeze and urban heat island effect. It is thus concluded that it is a very useful tool for local meteorological air pollution applications. Finally, some practical aspects of the future use of TAPM are commented and several useful tools for post-processing were developed and presented.

1. Background

Mathematical models are powerful tools for studying meteorology, air pollution problems and emission control strategies. Until now, there have been many air quality models developed for different scales ranging from local to urban to regional and global scales. On urban to regional scale, established air quality models, such as RADM, ADOM, STEM, RAINS-ASIA, CALGRID/CALPUFF, MODELS3, have been developed by different research groups in the world. However, most of these models have relatively coarse spatial resolutions and are difficulty to be applied for long-term simulations due to the complex physical and chemical processes involved.

Recently, TAPM (The Air Pollution Model) developed by Australian CSIRO Atmospheric Research Division appeared as an attractive model system since it integrates meteorology and air chemistry (Hurley, 1999b). This model was designed to be run in a nestable way so that the spatial resolution can be as fine as ~100 m. In addition, it can be run for one year or longer, which provides a means to deal with statistics of meteorological and pollutant variables.

TAPM has been used and verified for regions in Australia and other parts in the world (e.g. Hurley, 1999a). CSIRO has applied the model to meteorological (and some air pollution) verification studies for Kwinana and the Pilbara (WA), Cape Grim and Launceston (TAS) (Hurley, 1999a), Melbourne (VIC), Newcastle and Sydney (NSW), and Mt Isa (QLD), as well as for Kuala Lumpur (Malaysia). However, to our knowledge, use of TAPM in Europe has not been documented before. For its wide application in environmental impact assessment in Europe and in Sweden, it is necessary to perform a model validation using the observational data. In this report, a comparison will be made between the model results and the measurement to quantify TAPM's ability and performance for Sweden.

2. Description of the model system

2.1 Essentials of the Model

Air pollution models that can be used to predict pollution concentrations for periods of up to a year, are generally semi-empirical/analytic approaches based on Gaussian plumes or puffs. Typically, these models use either observed data from a surface based meteorological station or a diagnostic wind field model based on available observations. TAPM is different from these approaches in that it solves the fundamental fluid dynamics and scalar transport equations to predict meteorology and pollutant concentration for a range of pollutants important for air pollution applications. It consists of coupled prognostic meteorological and air pollution concentration components, eliminating the need to have site-specific meteorological observations.

Instead, the model predicts the flows important to local-scale air pollution transport, such as sea breezes and terrain induced flows, against a background of larger-scale meteorology provided by synoptic analyses. It predicts meteorological and pollution parameters directly (including photochemistry) on local, city or inter-regional scales. Its output can also be used to drive regulatory models such as ISC, AUSPLUME, DISPMOD, and AUSPUFF.

2.2. Meteorology model

The meteorological component of TAPM is an incompressible, non-hydrostatic, primitive equation model with a terrain-following vertical coordinate for three-dimensional simulations. The model solves the momentum equations for horizontal wind components, the incompressible continuity equation for vertical velocity, and scalar equations for potential virtual temperature and specific humidity of water vapour, cloud water and rainwater. Explicit cloud microphysical processes are included. Turbulence kinetic energy and eddy dissipation rate are calculated for determining the turbulence terms and the vertical fluxes. Further, surface energy budget is considered to computer the surface temperature. A vegetative canopy and soil scheme is used at the surface. Radiative fluxes at the surface and at upper levels are also calculated.

2.3. Air pollution model

The air pollution component of TAPM, which uses predicted meteorology and turbulence from the meteorological component, includes three modules. The Eulerian Grid Module (EGM) solves prognostic equations for concentration and for cross-correlation of concentration and virtual potential temperature. The Lagrangian Particle Module (LPM) can be used to represent near-source dispersion more accurately, while the Plume Rise Module is used to account for plume momentum and buoyancy effects for point sources. The model also has gas-phase photochemical reactions based on the Generic Reaction Set, and gas- and aqueous-phase chemical reactions for sulphur dioxide and particles. In addition, wet and dry deposition effects are also included.

2.4. Graphical user interface

The model is driven by a graphical user interface, which is used to (1) select all model input and configuration options, including access to supplied databases of terrain height, vegetation and soil type (USGS), synoptic-scale meteorology (CSIRO), and sea-surface temperature (NOAA); (2) run the model; (3) choose and process model output, including options for visualisation, extraction of time-series, production of static 1-D and 2-D plots and summary statistics using common packages such as EXCEL.

3. Validation of the model system

3.1. Model set-up and methodology

Since meteorological factors play an important role in air pollution modeling, it is necessary to verify the model's performance on meteorology modeling first. For this purpose, TAPM was run with three nestings that have spatial resolution of 9 km, 3 km and 1 km. There are 90*90 grid points in horizontal dimensions (see Figure 1) and 20 levels in vertical (10, 50, 100, 150, 200, 300, 400, 500, 750, 1000, 1250, 1500, 2000, 2500, 3000, 4000, 5000, 6000, 7000, and 8000 meters). The model was integrated for conseqtive five-day intervals covering the years 1999 and 2000. This approach is chosen because 1) the output for five days can be saved in one CD, which makes the output data manageable; 2) the five day simulation takes about two days for a normal PC to run, which is a reasonable time interval. A disadvantage with this approach is that the simulation is interrupted every five days, which implies that the small-scale variations may not be well developed in the beginning of every five-day simulation. Therefore, the model performance could well be better if the simulated data in the beginning (say the first day) would have been ignored.

The modeled air temperature at 2 m and wind at 10 m were selected as the two important fields for model validation. These levels are named modeled surface temperature and modeled surface wind respectively. The conventional statistical measures were adopted to determine the difference and correlation between the modeled results and the measurements. All comparisons were made for 1999 and 2000 respectively, in order to determine eventual differences from year to year.

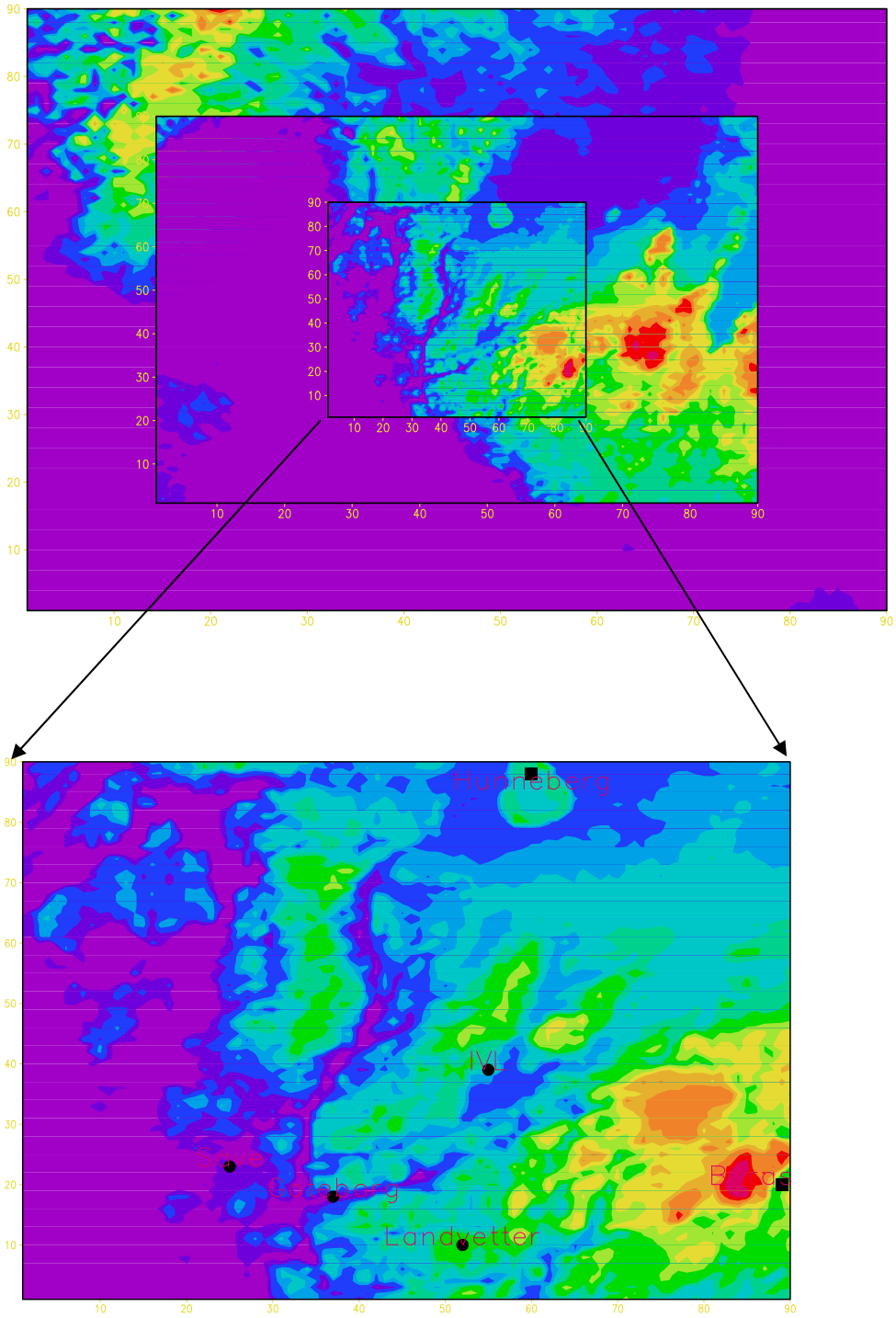

Figure 1. Model domains of the three nestings. The three surface stations (cycles) and two Sodar stations (squares) used in the comparisons are shown in the last nesting.

3.2. Observational Data

The observational data used for model validation are from NCDC/NOAA in the TD9956-Datsav III variable length ASCII format. The TD9956 data contain all hourly records as well as any observations taken between hours. It is probably the most complete data set as it contains all information transmitted by the station. For more information, one can visit the homepage at:

http://lwf.ncdc.noaa.gov/oa/climate/climatedata.html

http://lwf.ncdc.noaa.gov/oa/climate/climateinventories.html#ABOUT

http://lwf.ncdc.noaa.gov/oa/climate/surfaceinventories.html#A

To be able to carry out a comprehensive study, data from 50 Swedish meteorological stations with hourly values (or the best available time resolution) were collected. The details about the stations are listed in Table 1. The time period of the data is from 1 January 1999 to 31 December 2000. To limit the scope of this report, only three stations from Table 1 containing surface meteorological data were used for this report. They are GOTEBORG (Göteborg), LANDVETTER and SAVE (Säve), as indicated by bold letters. The three stations provides meteorological data from various levels above the ground (Göteborg ≈ 50 m, Landvetter ≈ 10 m and Säve ≈ 10 m) characterising the urban and suburban surface in the area. These levels are all named observed surface temperature and observed surface wind respectively.

Table 1. Information for 50 Swedish meteorological stations

NUMBER	CALL	NAME + COUNTRY/STATE	LAT	LON	ELEV(M.A.S.L)
024990		ALMAGRUNDET	SN	5909N	01908E 0025
026070	ESDB	ANGELHOLM (SWE-AFB)	SN	5618N	01251E 0047
024080		BLOMSKOG (AUTO)	SN	5913N	01205E 0171
024350	ESSD	BORLANGE (SWE-AFB)	SN	6026N	01531E 0161
024760		FLODA (AUTO)	SN	5903N	01624E 0020
024530		GAVLE	SN	6040N	01710E 0005
025130		**GOTEBORG**	**SN**	**5742N**	**01200E 0005**
025260	**ESGG**	**GOTEBORG/LANDVETTER**	**SN**	**5740N**	**01218E 0169**
025120	**ESGP**	**GOTEBORG/SAVE (AFB)**	**SN**	**5747N**	**01153E 0053**
025840		GOTSKA SANDON (LH)	SN	5824N	01912E 0012
025560	ESMV	HAGSHULT (SWE-AFB)	SN	5718N	01408E 0172
026050		HALLANDS VADERO\AUT	SN	5627N	01233E 0010
026040	ESMT	HALMSTAD (SWE-AFB)	SN	5641N	01250E 0030

026280		HANO (AUTO)	SN	5601N	01451E 0060
026110		HELSINGBORG	SN	5603N	01241E 0005
026800		HOBURG (LGT-H)	SN	5655N	01809E 0039
025500	ESGJ	JONKOPING AIRPORT	SN	5746N	01405E 0232
026720	ESMQ	KALMAR	SN	5644N	01618E 0016
024150	ESOK	KARLSTAD SOL	SN	5922N	01328E 0046
024180	ESSQ	KARLSTADT AIRPORT	SN	5922N	01328E 0055
026510	ESMK	KRISTIANSTAD/EVEROD	SN	5555N	01405E 0023
025670		LANDSORT (AUTO)	SN	5845N	01752E 0020
025625	ESSL	LINKOPING/SAAB	SN	5824N	01541E 0052
025660		MALILLA	SN	5724N	01550E 0098
026360	ESMS	MALMO/STURUP	SN	5533N	01322E 0106
025050		MASESKAR (AUT0)	SN	5806N	01120E 0016
025180		NIDINGEN (LGT-H)	SN	5718N	01154E 0005
025710	ESSP	NORRKOPING/KUNGSANG	SN	5835N	01609E 0008
025750		OLANDSNORRAUDDE\AUT	SN	5722N	01706E 0004
026440		OLANDSSODRAUDDE\AUT	SN	5612N	01624E 0003
024320		OREBRO (AUTO)	SN	5914N	01503E 0055
024283	ESOE	OREBRO (PRIVATE)	SN	5914N	01503E 0057
024880		ORSKAR (AUTO)	SN	6032N	01823E 0009
025360		RANGEDALA (AUTO)	SN	5747N	01310E 0299
026640	ESDF	RONNEBY (SWE-AFB)	SN	5616N	01517E 0074
025200	ESIB	SATENAS (SWE-AFB)	SN	5826N	01242E 0074
024853	ESKN	SKAVASTA/STOCKHOLM	SN	5847N	01655E 0043
026250		SKILLINGE (AUTO)	SN	5529N	01419E 0005
025350	ESGR	SKOVDE AIRPORT	SN	5827N	01358E 0105
024870		STAVSNAS	SN	5918N	01842E 0013
024600	ESSA	STOCKHOLM/ARLANDA	SN	5939N	01757E 0061
024640	ESSB	STOCKHOLM/BROMMA	SN	5921N	01757E 0011
024960		SVENSKA HOGARNA(LH)	SN	5927N	01930E 0012
026200		TORUP	SN	5658N	01306E 0085
025103	ESGT	TROLLHATTAN (PVT)	SN	5819N	01221E 0041
025170		TRUBADUREN	SN	5736N	01138E 0026
024580	ESCM	UPPSALA (SWE-AFB)	SN	5953N	01736E 0041

024460	ESOW	VASTERAS/HASSLO AFB	SN	5935N	01638E 0031
026410	ESMX	VAXJO/KRONOBERG	SN	5656N	01444E 0186
025900	ESSV	VISBY AIRPORT	SN	5740N	01821E 0047

In addition, upper level wind data from two sound radar stations (Hunneberg, Borås) were selected for profiles comparisons. Compared with the surface data, the Sodar data is rather incomplete. The wind profiles are measured by two Sensitron AQ-system sodar, Stockholm AB, Sweden, who works like an acoustic radar transmitting sound pulses which are reflected by the temperature structure in the air. By detecting signals from the reflected Doppler-shifted sound, the sodar system can derive and present information on the vertical wind profile. The instruments provides wind profiles from 50 m height up to maximum 475 m height. Generally, data is collected up to a level of approximately 175 m but very seldom above 400 m. The horizontal wind range is 35 m/s, the vertical wind range is ±10 m/s. The wind accuracy is 0.2 m/s or better for the horizontal and 0.05 m/s for the vertical wind.

To make the direct comparison possible, sodar measurements at different levels are interpolated to the model levels. Missing values appear in both the surface and upper air measurement osccasionallly. Simulated values are ommited if the corresponding observations are missing. Thus, the numbers of data available for different comparisons vary always and need to be indicated in the statistics.

4.Results

4.1. Surface comparison

The scatter plots of the observed and modelled hourly near ground air temperature, horizontal wind (u, v component) at the three surface stations are displayed in Figures 2-4 for 1999 and for 2000 respectively. The related statistics can be found in Table 2.

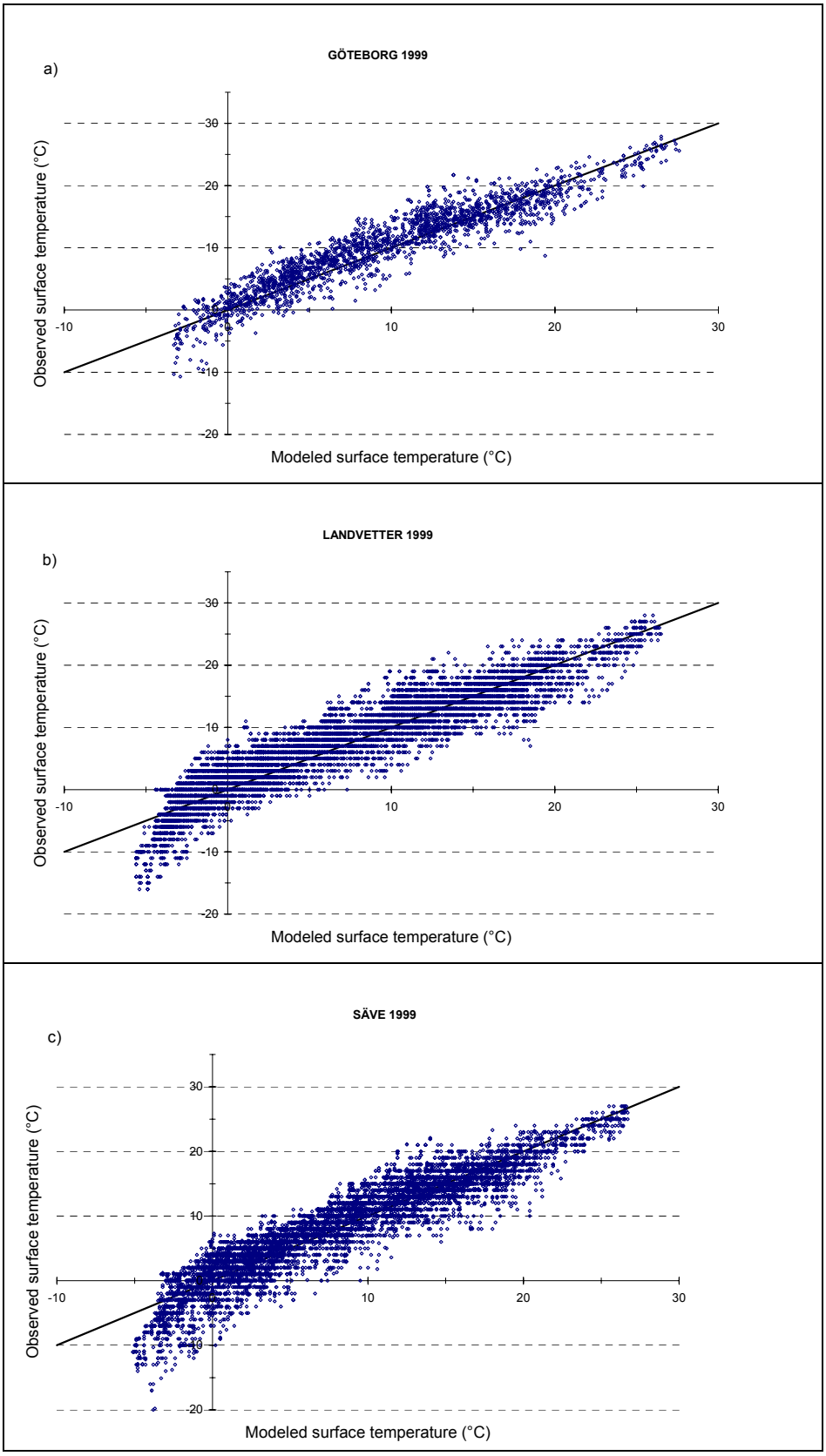
GÖTEBORG 1999
a)
Observed surface temperature (°C)
Modeled surface temperature (°C)
-10
10
20
30
-20
LANDVETTER 1999
b)
Observed surface temperature (°C)
Modeled surface temperature (°C)
SÄVE 1999
c)
Observed surface temperature (°C)
Modeled surface temperature (°C)

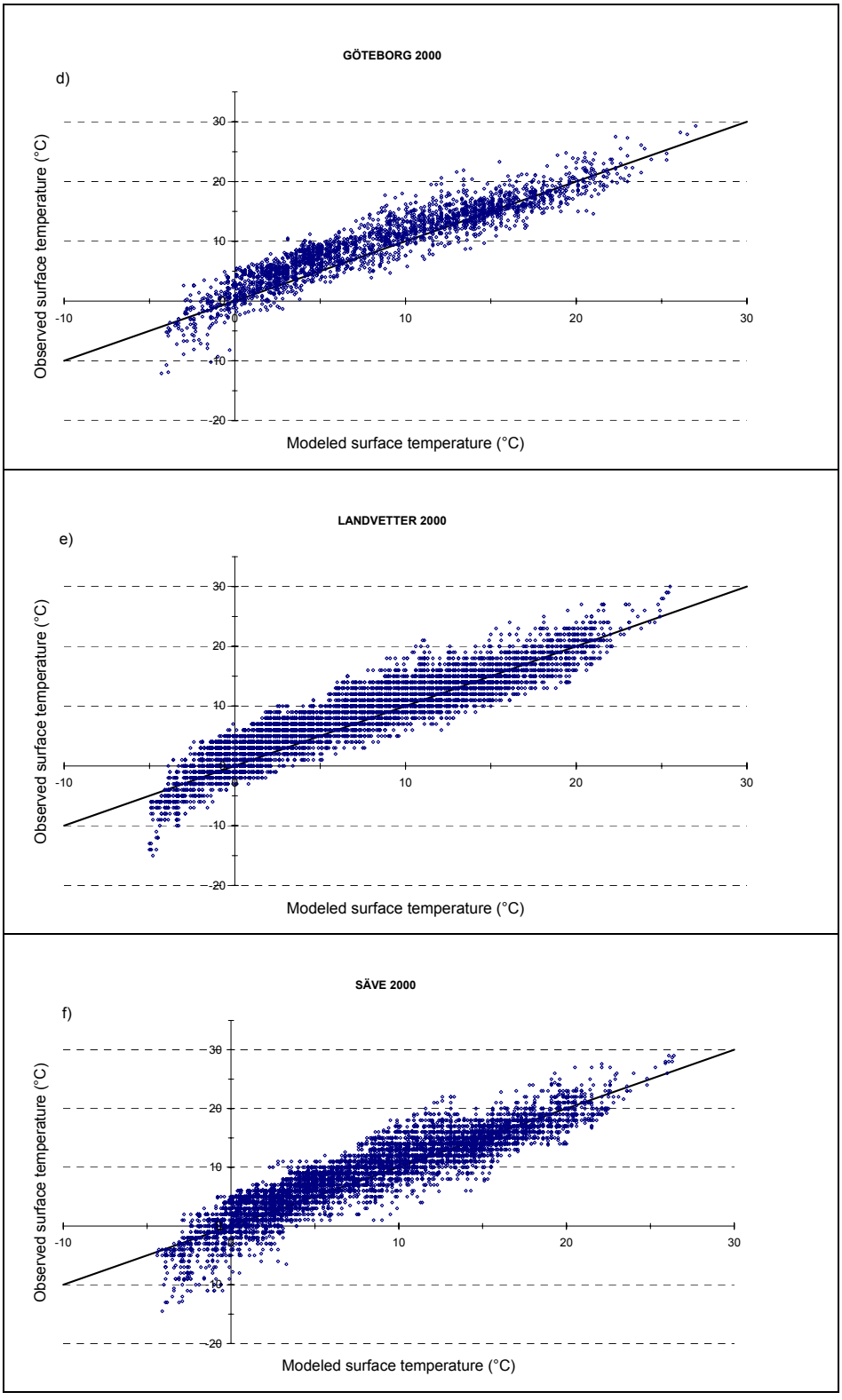

Figure 2. Scatter plot of the observed and modeled hourly surface air temperature at three surface stations for 1999 (a, b, c) and for 2000 (d, e, f) respectively.

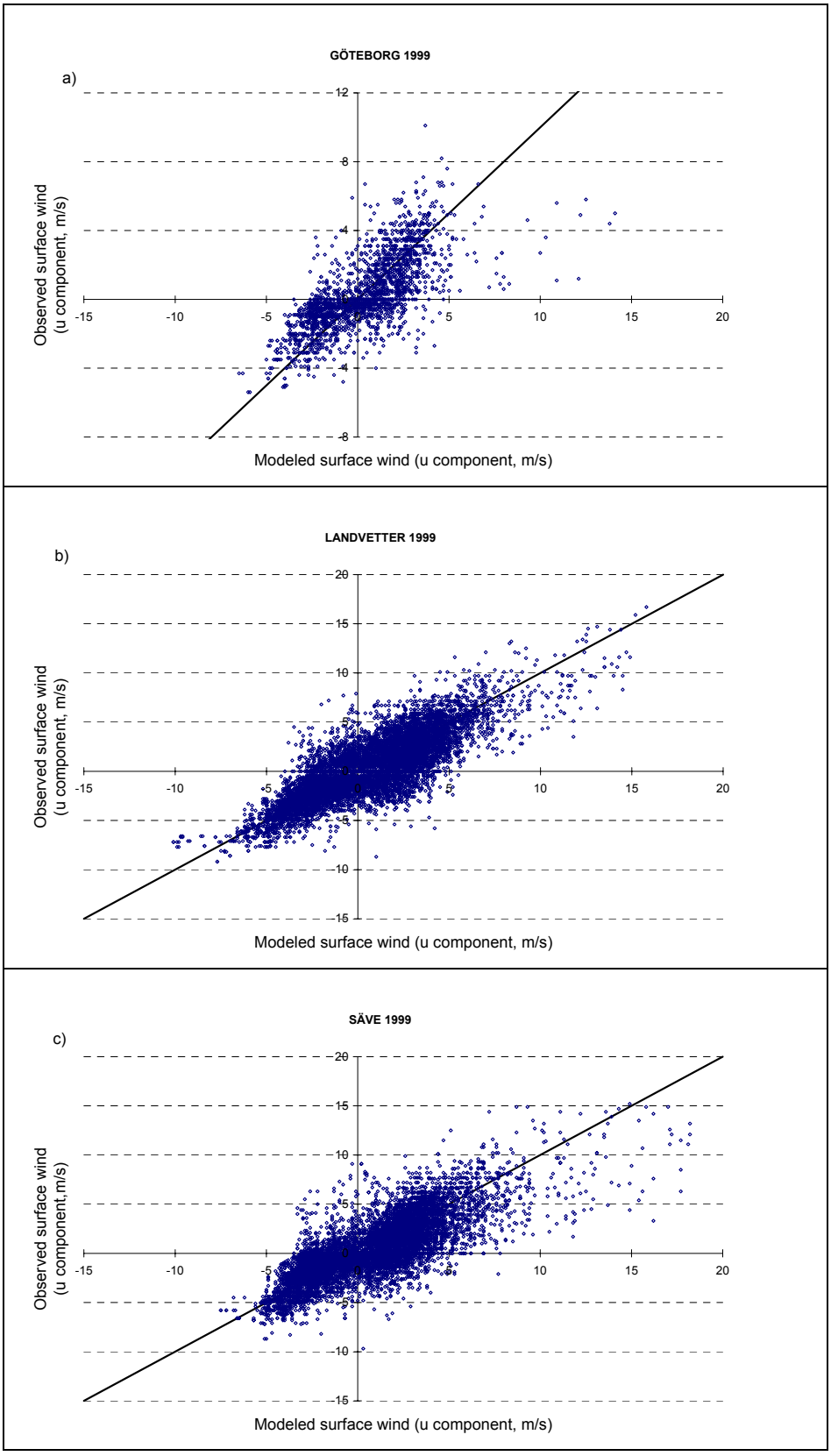
GÖTEBORG 1999
a)
Observed surface wind (u component, m/s)
Modeled surface wind (u component, m/s)
LANDVETTER 1999
b)
Observed surface wind (u component, m/s)
Modeled surface wind (u component, m/s)
SÄVE 1999
c)
Observed surface wind (u component,m/s)
Modeled surface wind (u component, m/s)

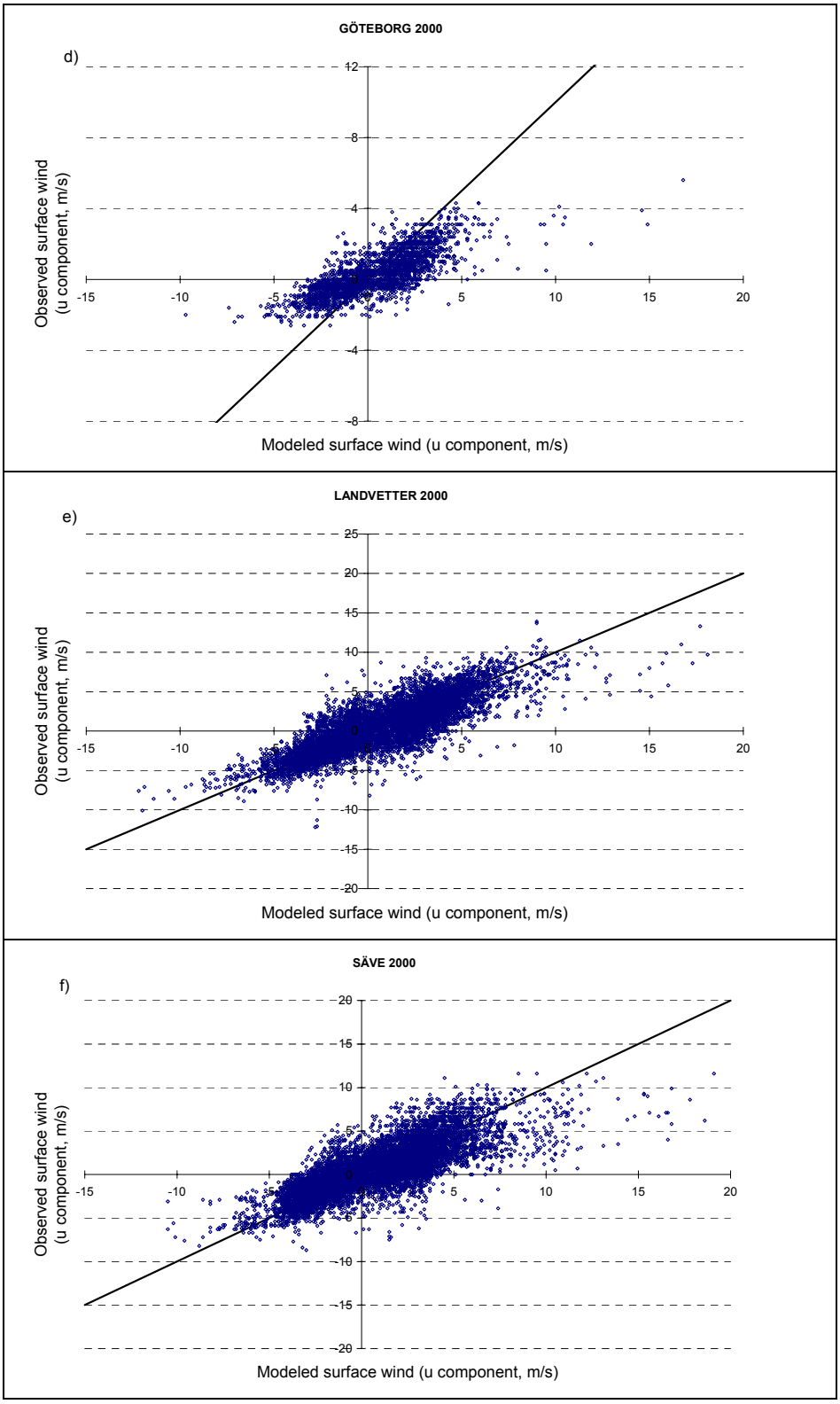

Figure 3. Scatter plot of the observed and modeled hourly surface wind (u component) at three surface stations for 1999 (a, b, c) and for 2000 (d, e, f) respectively.

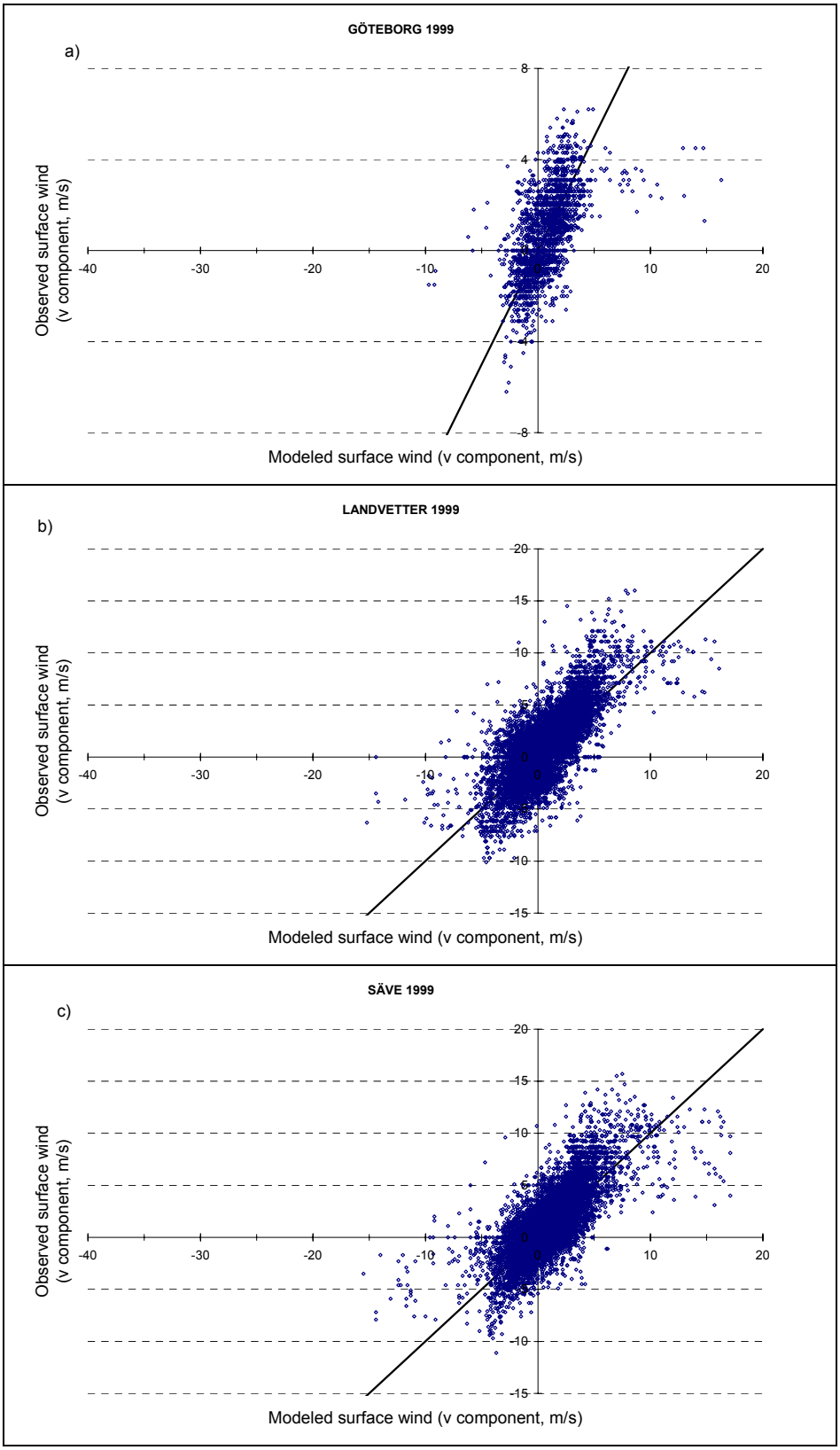
GÖTEBORG 1999
a)
Observed surface wind (v component, m/s)
Modeled surface wind (v component, m/s)
LANDVETTER 1999
b)
Observed surface wind (v component, m/s)
Modeled surface wind (v component, m/s)
SÄVE 1999
c)
Observed surface wind (v component, m/s)
Modeled surface wind (v component, m/s)

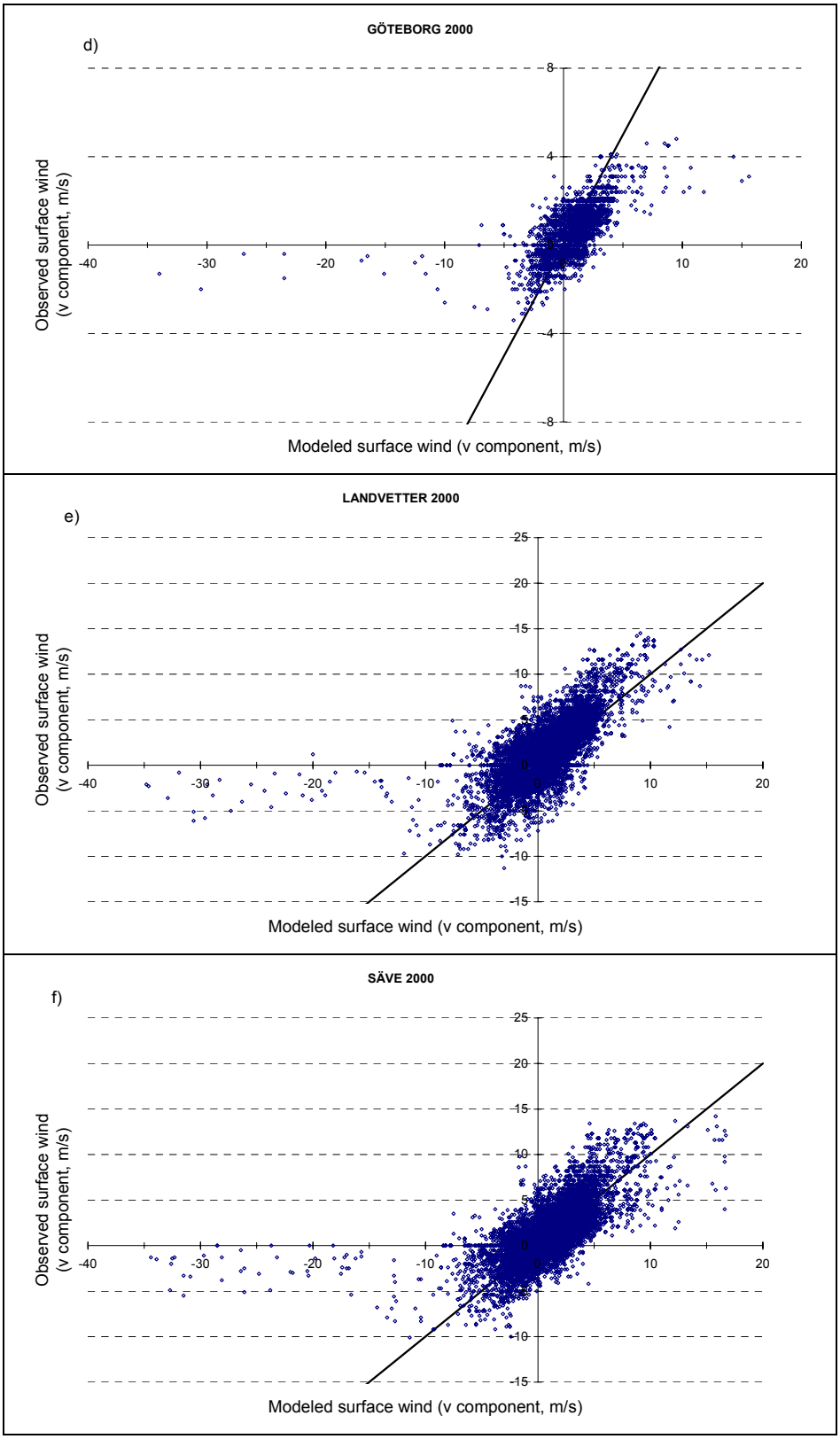

Figure 4. Scatter plot of the observed and modeled hourly surface wind (v component) at three surface stations for 1999 (a, b, c) and for 2000 (d, e, f) respectively.

The statistics listed in the tables 2a and 2b, shows that TAPM has been successfully in modeling the near surface temperature and horizontal wind, although the skills for temperature and wind are varying. For surface temperature, high correlation (greater than 0.92) and small square error (0.03 to 0.05 ^{o}C) were found between the model results and the measurements. The surface wind was also well simulated, but the correlation coefficient is somewhat lower compared to those of temperature. In general, the model systematically underestimated surface temperature by about 1 ^{o}C. As to the horizontal wind, it was overestimated at urban site (Göteborg) and underestimated at non-urban sites (Landvetter as well as Säve) in 1999. There is a considerable changes in the statistics from 1999 to 2000, indicating year-to-year change is something important for this region.

Table 2(a). Comparison between the modeled and observed variables for 1999

	Correlation coefficient	*Modeled average*	*Observed average*	*Bias*	*RMSE*
(a)Göteborg (2085*)					
Surface air temperature (^{o}C)	0.94	9.8	10.4	-0.6	0.2
Surface wind u component (m/s)	0.71	0.4	0.3	0.1	0.2
Surface wind v component (m/s)	0.60	0.7	0.7	0.0	0.2
Surface wind speed (m/s)	0.38	2.8	2.5	0.3	0.2
(b) Landvetter (8711)					
Surface air temperature (^{o}C)	0.93	6.9	7.6	-0.7	0.2
Surface wind, u component (m/s)	0.82	0.7	0.4	0.3	0.2
Surface wind, v component (m/s)	0.75	1.0	1.6	-0.6	0.2
Surface wind speed (m/s)	0.67	3.9	4.4	-0.5	0.2
(c) Säve (8765)					
Surface air temperature (^{o}C)	0.94	7.9	8.2	-0.3	0.2
Surface wind, u component (m/s)	0.78	0.8	0.6	0.2	0.2
Surface wind, v component (m/s)	0.75	1.1	1.4	-0.3	0.2
Surface wind speed (m/s)	0.65	3.9	4.1	-0.2	0.2

* sample number for statistics

Table 2(b). Comparison between the modeled and observed variables for 2000

	Correlation coefficient	*Modeled average*	*Observed average*	*Bias*	*RMSE*
(a) Göteborg (2695*)					
Surface air temperature (^{o}C)	0.94	7.8	9.3	-1.5	0.2
Surface wind, u component (m/s)	0.78	0.6	0.4	0.2	0.2
Surface wind, v component(m/s)	0.64	0.8	0.6	0.2	0.2
Surface wind speed (m/s)	0.52	3.0	1.6	1.4	0.2
(b) Landvetter (8585)					
Surface air temperature (^{o}C)	0.93	6.4	7.7	-1.3	0.2
Surface wind, u component (m/s)	0.85	1.0	0.9	0.1	0.1
Surface wind, v component (m/s)	0.71	1.0	2.0	-1.0	0.2
Surface wind speed (m/s)	0.61	4.3	4.7	-0.4	0.2
(c) Säve (10347)					
Surface air temperature (^{o}C)	0.92	7.4	8.5	-1.1	0.2
Surface wind, u component (m/s)	0.79	1.1	0.9	0.2	0.1
Surface wind, v component (m/s)	0.69	1.2	1.6	-0.4	0.2
Surface wind speed (m/s)	0.55	4.2	4.0	0.2	0.2

* sample number for statistics

The diurnal, seasonal variations and daily averages of the observed and simulated surface temperature are presented in Figures 5-7 for 1999 and 2000 respectively. The underestimate of the surface temperature in Göteborg appears to be systematic with respect to time, as shown by Figures 5a and 5d. This is especially true for 2000. However, the seasonal variations as shown by Figure 5e indicate that the underestimates mainly occur in could months. This may be partly due to the neglect of the anthropogenic heating in the city. For Landvetter the underestimate mainly appears during the day (Figure 6a) even if the year-to-year change can be large (Figure 6a and Figure 6d). Once again, cold months have a larger underestimate than the warm months (Figure 6b and Figure 6e). Simulations for Säve (Figure 7) show a similar pattern as Göteborg and Landvetter.

The diurnal, seasonal variations and daily averages of the observed and simulated surface wind direction (Figures 8-10) and speed are displayed in Figures 11-13 for 1999 and 2000 respectively. In general, the simulations for wind direction follow the evolution of the observation well, although there are fairly systematic differences. For

wind speed, the differences between 1999 and 2000 can be fairly large specially for Göteborg (Figure 11d).

The model has a strong ability to simulate urban heat island effect, which can be seen in Figure 14. The figure shows that the temperature difference between the urban (Göteborg) and the suburb (Landvetter and Säve) stations can reach 1.4-3.4 ºC (Göteborg-Landvetter) and 1.5-3.8 ºC) (Göteborg-Säve) on the hourly basis for modeled results and for measurements. The simulations follow the observations well, though the difference varies with year.

A very important feature of TAPM is its ability to explicitly deal with surface energy budget and temperature, which allows simulation of thermally driven wind systems. An examination of the modeled results reveals that the model performs well in modeling mesoscale wind system, such as land-sea breeze circulation. As an example, Figures 15-18 display a simulation of such a wind system during 1999 in various ways.

The figures show that during the daytime, solar radiation heats the ground faster than the sea, which results in the higher air temperature over the land compared to the sea. Therefore, air with lower density goes up over the land and air with higher density goes down over the sea. Near the surface, air flow from the sea to the land, leading to the sea breeze. During the night, the cooling of the land is faster than the sea, hence air blow from the land to the sea over the surface, leading the formation of land breeze. The return flow of the sea breeze can be seen (Figure 17b) at the model level 9 (750 m).

4.2 Profile comparison

The statistics of observed and modelled wind profile at selected levels at Hunneberg and Borås are listed in Table 3 and Table 4, respectively. Following features are obvious: 1) The evolution of the simulated upper winds follow those of the observed fairly well, as reflected in the correlation coefficients that are comparable to those in the surface comparison; 2) the agreements at the two sites are comparable; 3) the Sodar measurements at the two sites have a persistent bias, pointing to a systematic error in the measurement; 4) difference between results in 1999 and 2000 are considerable, with results in 2000 being worse than those in 1999. One possible reason could be poorer quality of synoptic data in 2000.

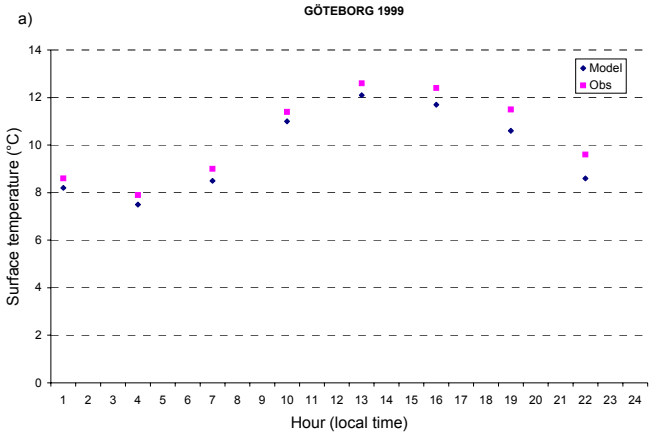
a)
GÖTEBORG 1999
Surface temperature (°C)
Hour (local time)
Model
Obs

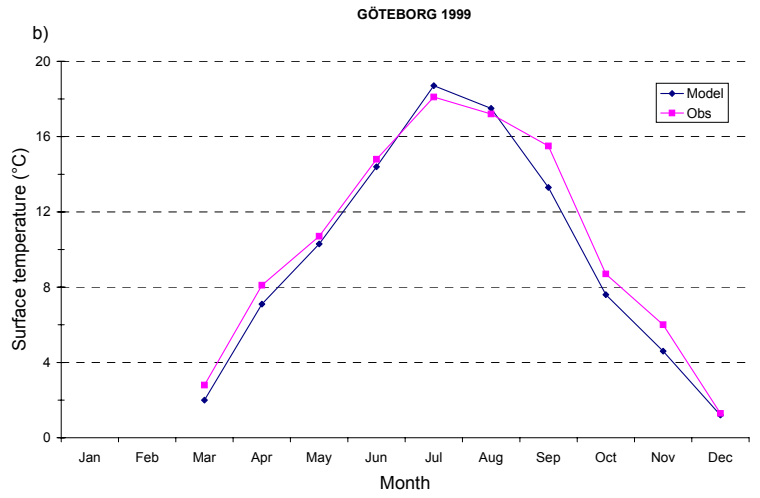
b)
GÖTEBORG 1999
Surface temperature (°C)
Month
Jan
Feb
Mar
Apr
May
Jun
Jul
Aug
Sep
Oct
Nov
Dec
Model
Obs

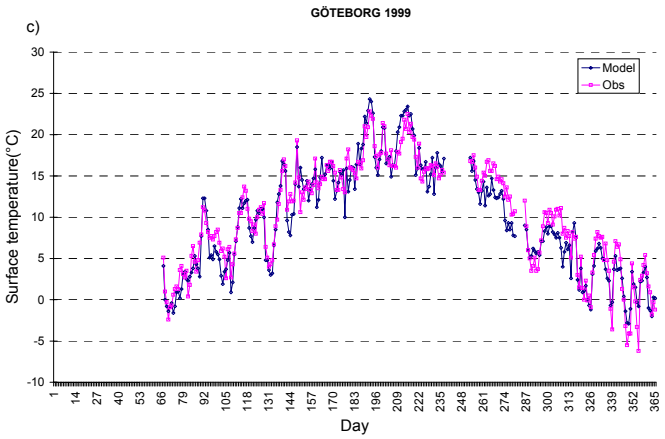
c)
GÖTEBORG 1999
Surface temperature(°C)
Day
Model
Obs

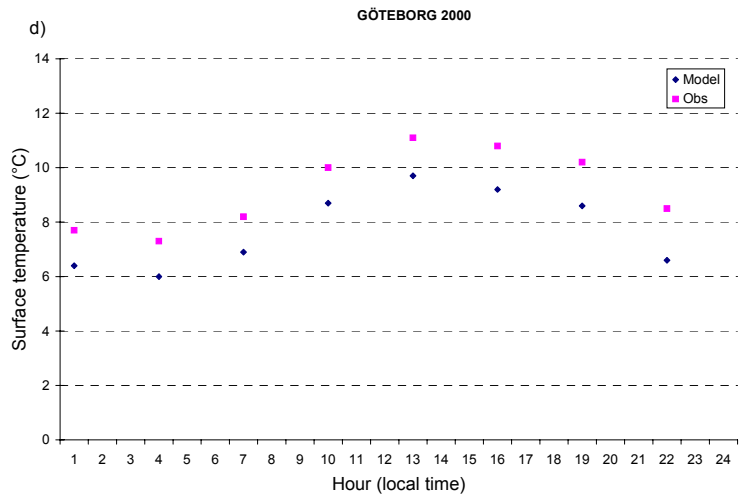
d)
GÖTEBORG 2000
Surface temperature (°C)
Hour (local time)
Model
Obs

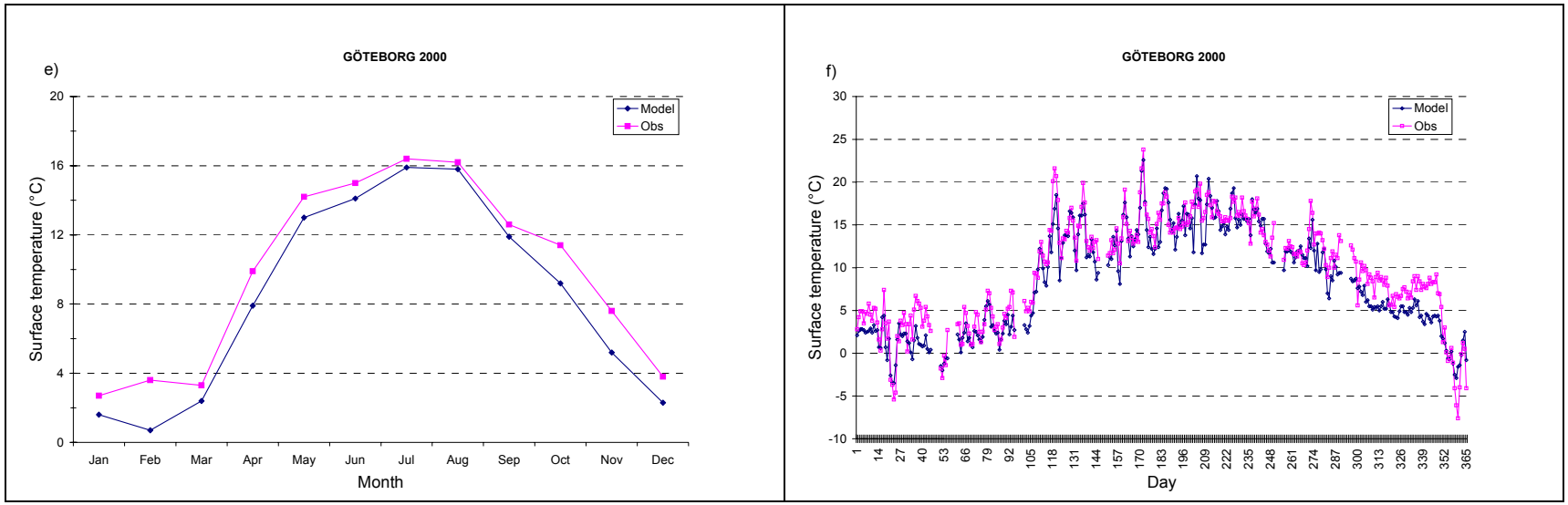

Figure 5. The observed and modeled surface air temperature at Göteborg for 1999 and for 2000 respectively (a, d) diurnal variation; (b, e) seasonal variation; (c, f) daily average.

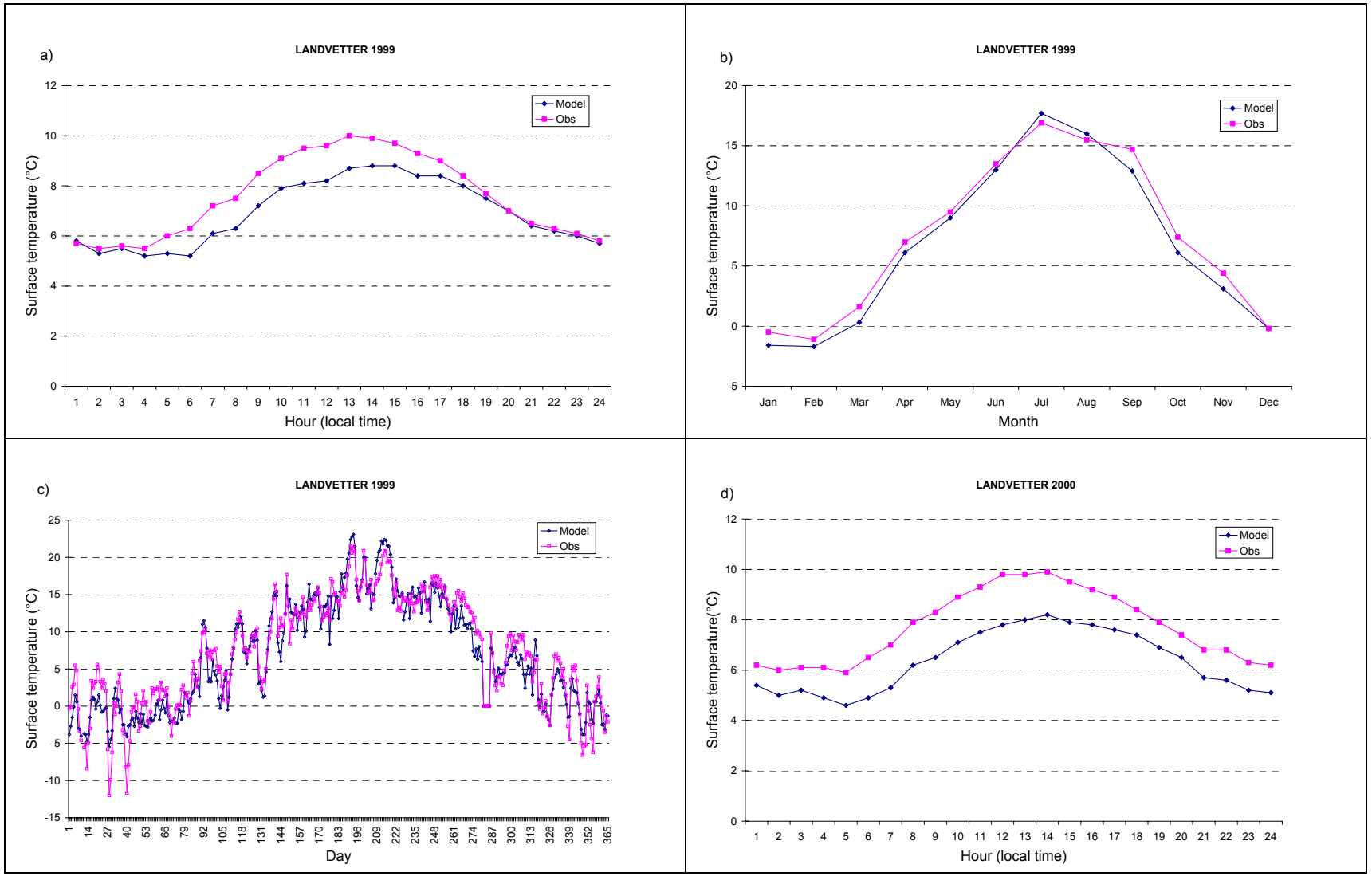
a)
LANDVETTER 1999
Model
Obs
Surface temperature (°C)
Hour (local time)
b)
LANDVETTER 1999
Model
Obs
Surface temperature (°C)
Jan
Feb
Mar
Apr
May
Jun
Jul
Aug
Sep
Oct
Nov
Dec
Month
c)
LANDVETTER 1999
Model
Obs
Surface temperature (°C)
Day
d)
LANDVETTER 2000
Model
Obs
Surface temperature(°C)
Hour (local time)

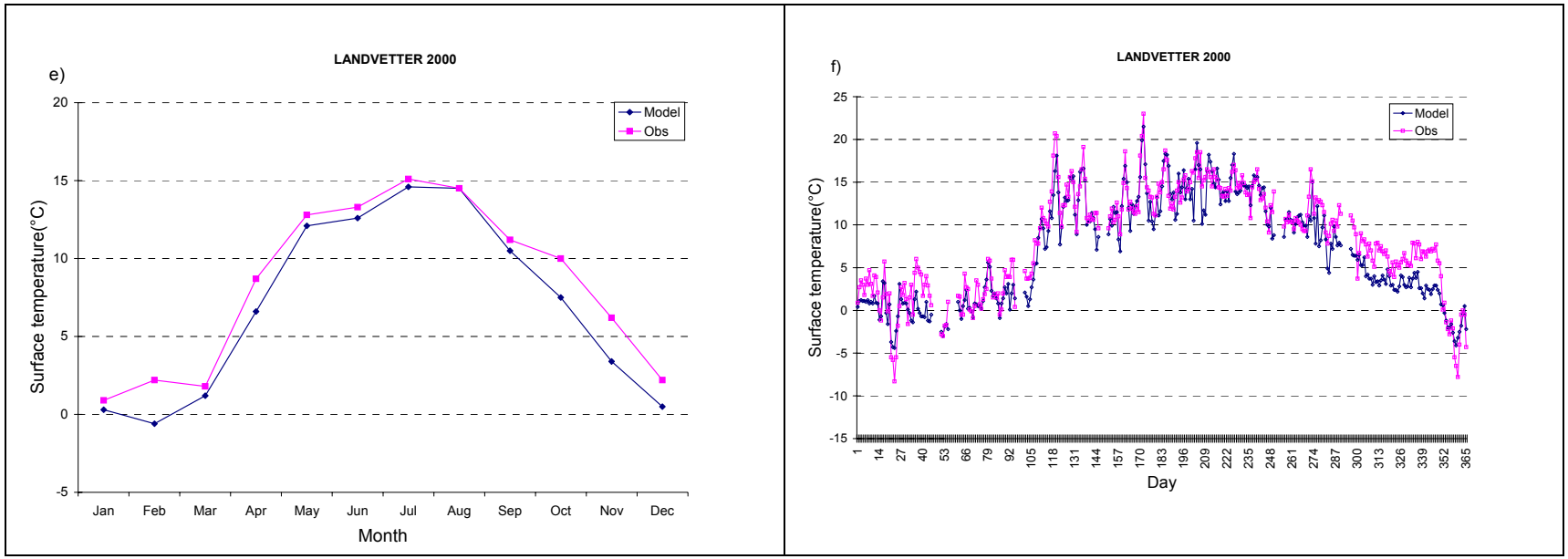

Figure 6. The observed and modeled surface air temperature at Landvetter for 1999 and for 2000 respectively (a, d) diurnal variation; (b, e) seasonal variation; (c, f) daily average.

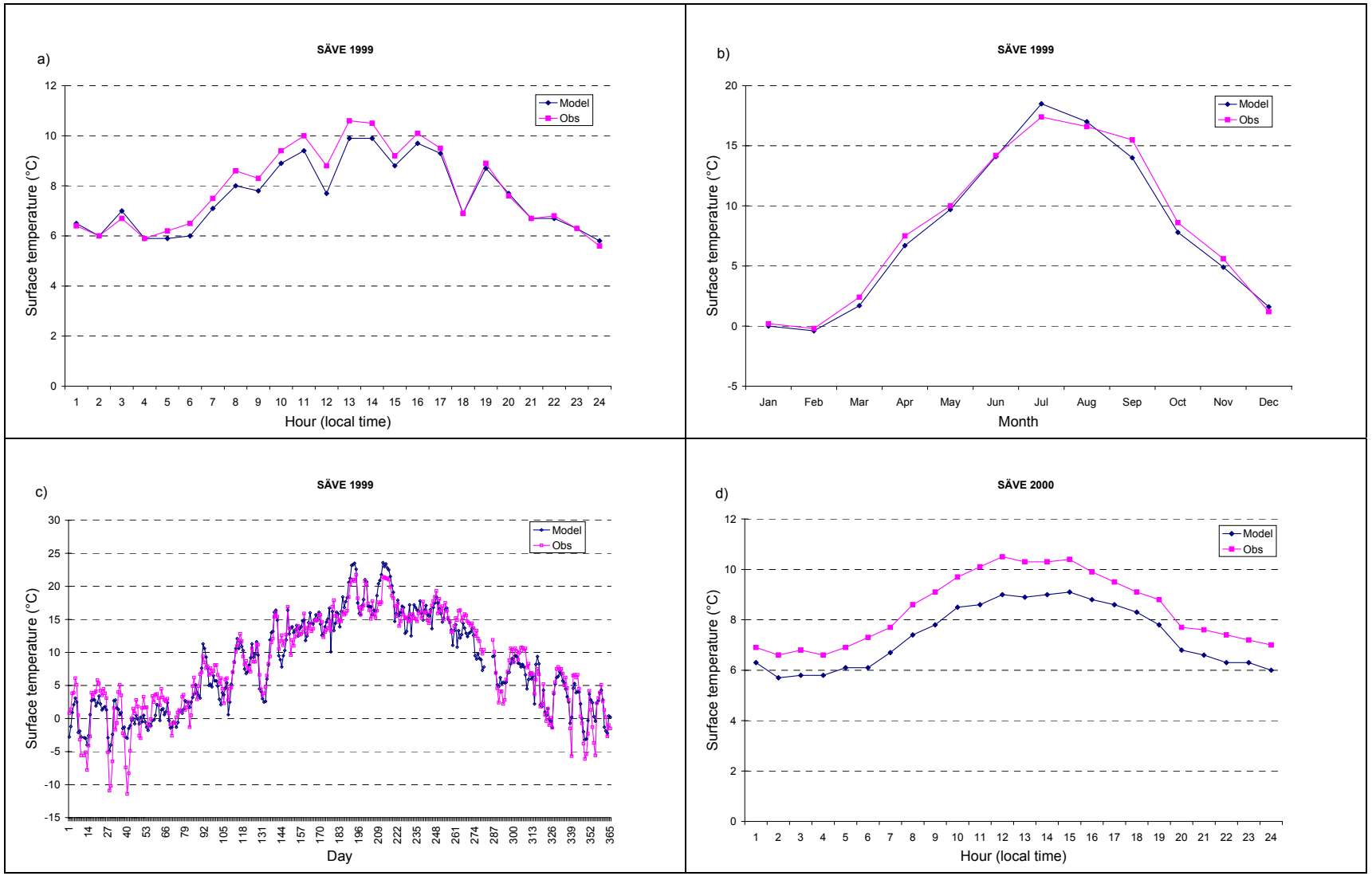
a)
SÄVE 1999
Surface temperature (°C)
Hour (local time)
Model
Obs
b)
SÄVE 1999
Surface temperature (°C)
Month
Jan
Feb
Mar
Apr
May
Jun
Jul
Aug
Sep
Oct
Nov
Dec
Model
Obs
c)
SÄVE 1999
Surface temperature (°C)
Day
Model
Obs
d)
SÄVE 2000
Surface temperature (°C)
Hour (local time)
Model
Obs

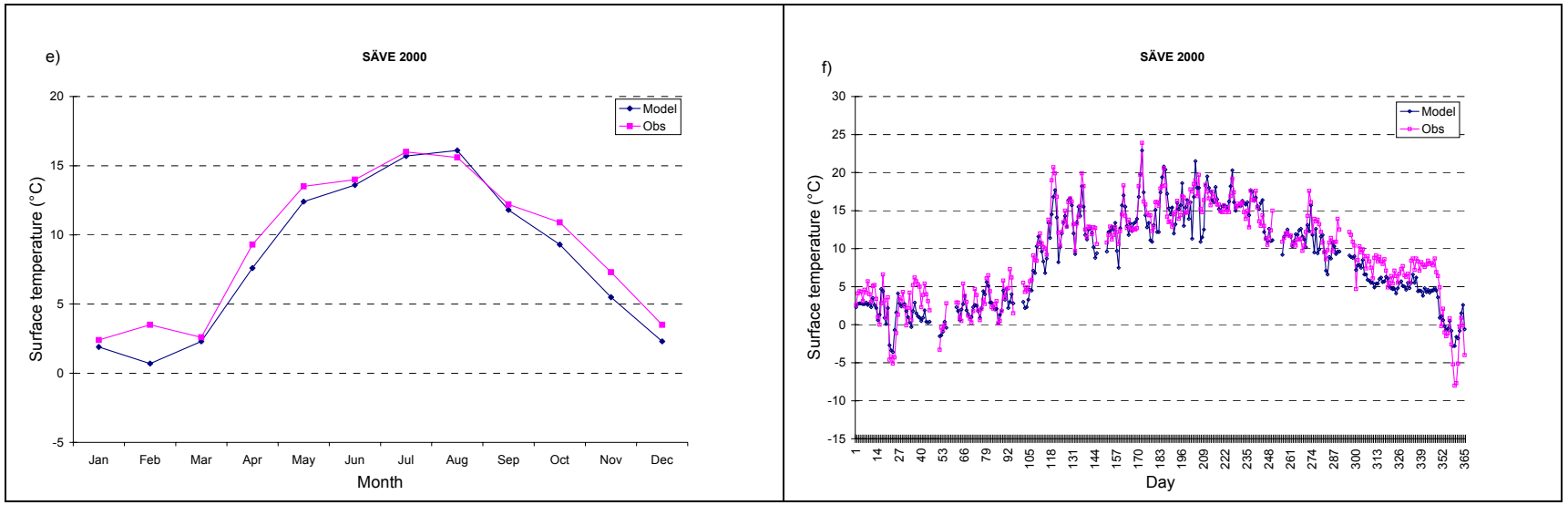

Figure 7. The observed and modeled surface air temperature at Säve for 1999 and for 2000 respectively (a, d) diurnal variation; (b, e) seasonal variation; (c, f) daily average.

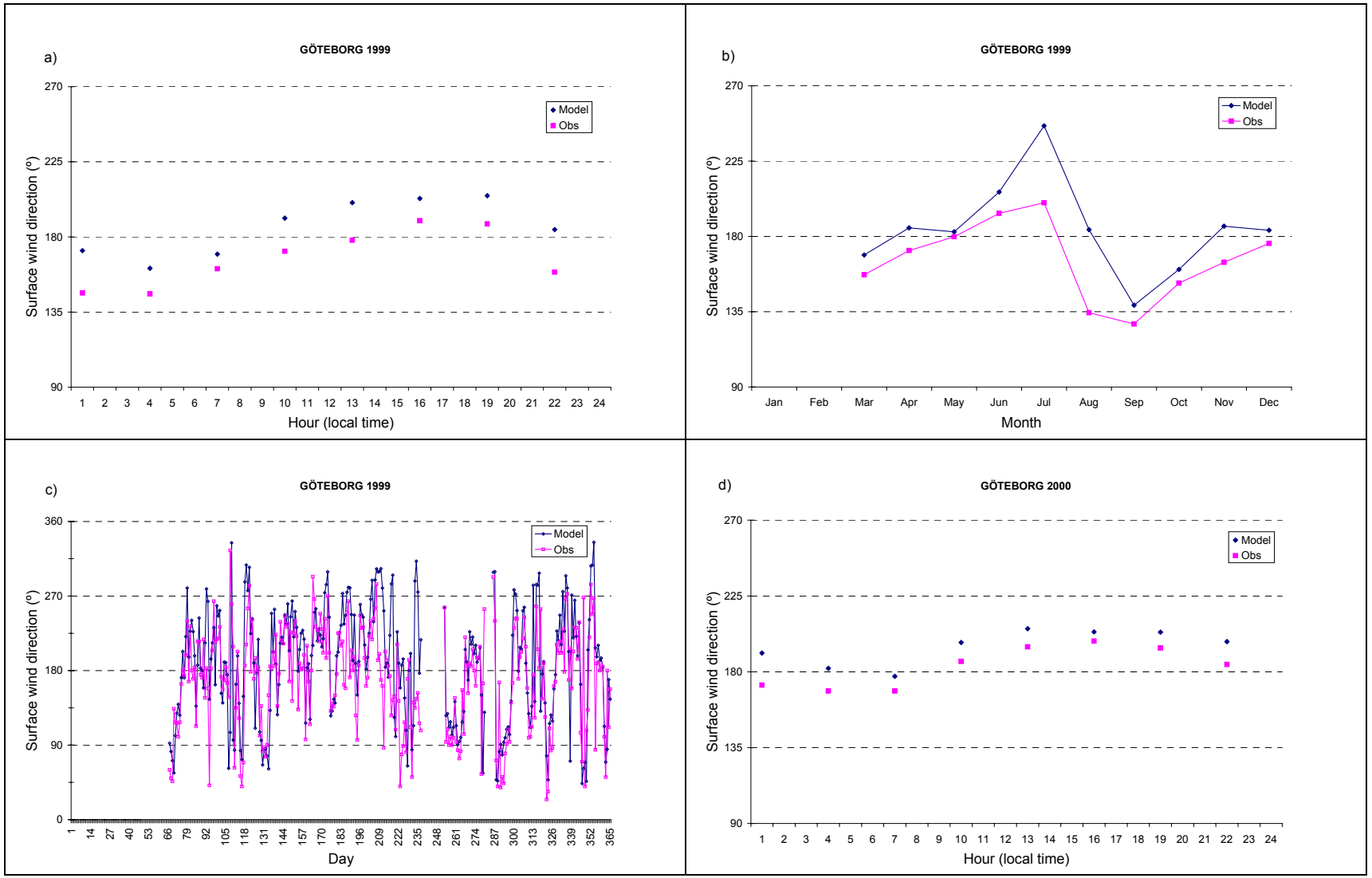
a)
GÖTEBORG 1999
Surface wind direction (°)
270
225
180
135
90
Model
Obs
1 2 3 4 5 6 7 8 9 10 11 12 13 14 15 16 17 18 19 20 21 22 23 24
Hour (local time)
b)
GÖTEBORG 1999
Surface wind direction (°)
270
225
180
135
90
Model
Obs
Jan Feb Mar Apr May Jun Jul Aug Sep Oct Nov Dec
Month
c)
GÖTEBORG 1999
Surface wind direction (°)
360
270
180
90
0
Model
Obs
1 14 27 40 53 66 79 92 105 118 131 144 157 170 183 196 209 222 235 248 261 274 287 300 313 326 339 352 365
Day
d)
GÖTEBORG 2000
Surface wind direction (°)
270
225
180
135
90
Model
Obs
1 2 3 4 5 6 7 8 9 10 11 12 13 14 15 16 17 18 19 20 21 22 23 24
Hour (local time)

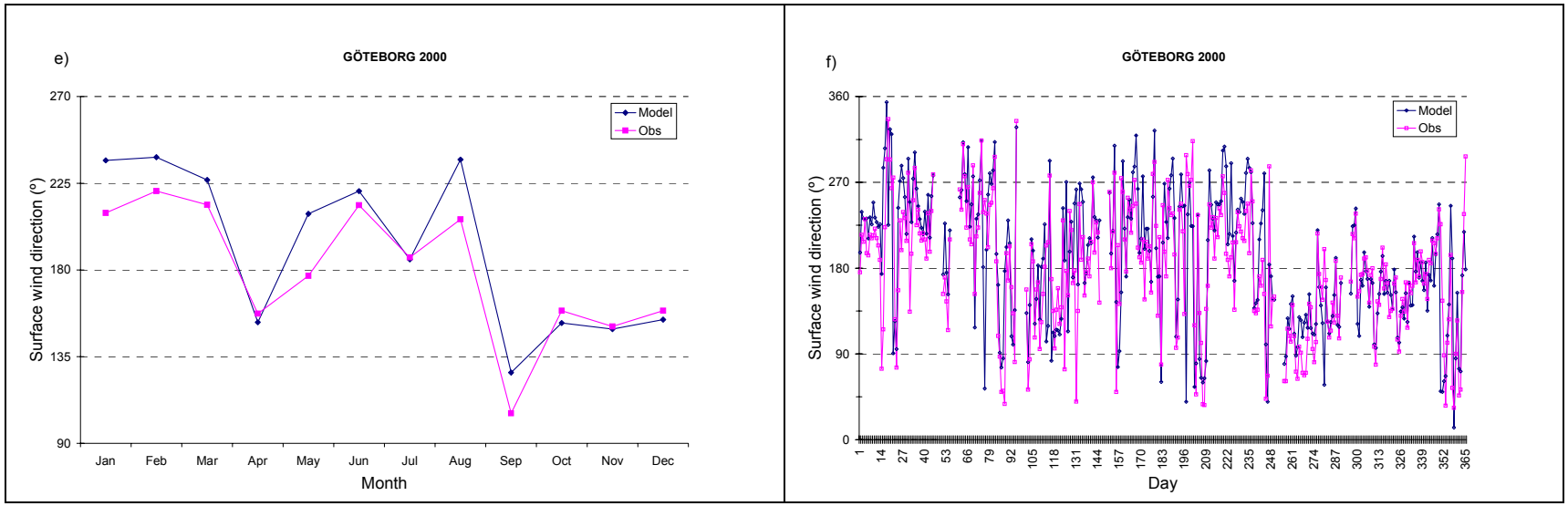

Figure 8. The observed and modeled surface wind direction at Göteborg for 1999 and for 2000 respectively (a, d) diurnal variation; (b, e) seasonal variation; (c, f) daily average.

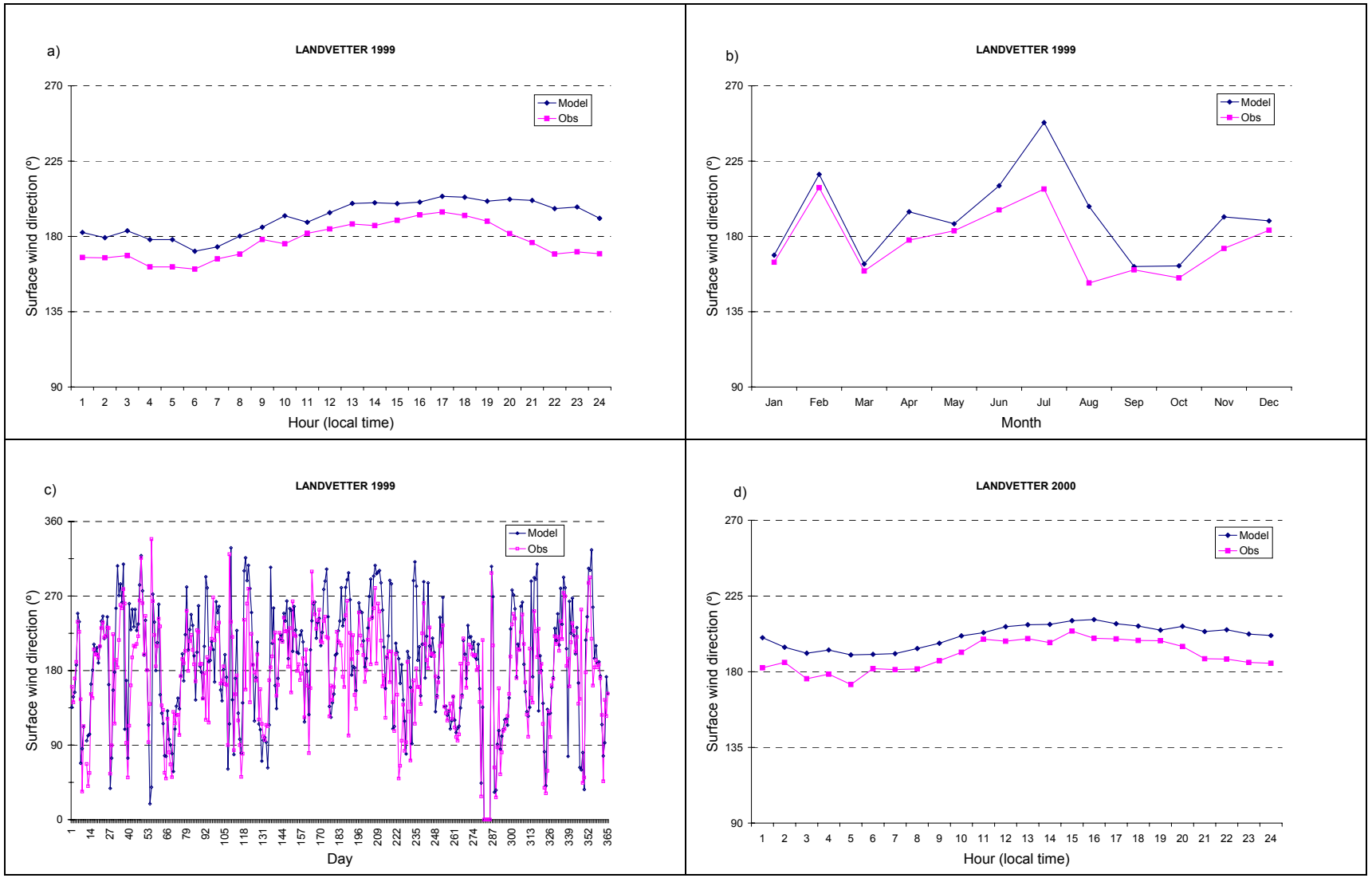
a)
LANDVETTER 1999
Model
Obs
Surface wind direction (°)
270
225
180
135
90
1 2 3 4 5 6 7 8 9 10 11 12 13 14 15 16 17 18 19 20 21 22 23 24
Hour (local time)
b)
LANDVETTER 1999
Model
Obs
Surface wind direction (°)
270
225
180
135
90
Jan Feb Mar Apr May Jun Jul Aug Sep Oct Nov Dec
Month
c)
LANDVETTER 1999
Model
Obs
Surface wind direction (°)
360
270
180
90
0
1 14 27 40 53 66 79 92 105 118 131 144 157 170 183 196 209 222 235 248 261 274 287 300 313 326 339 352 365
Day
d)
LANDVETTER 2000
Model
Obs
Surface wind direction (°)
270
225
180
135
90
1 2 3 4 5 6 7 8 9 10 11 12 13 14 15 16 17 18 19 20 21 22 23 24
Hour (local time)

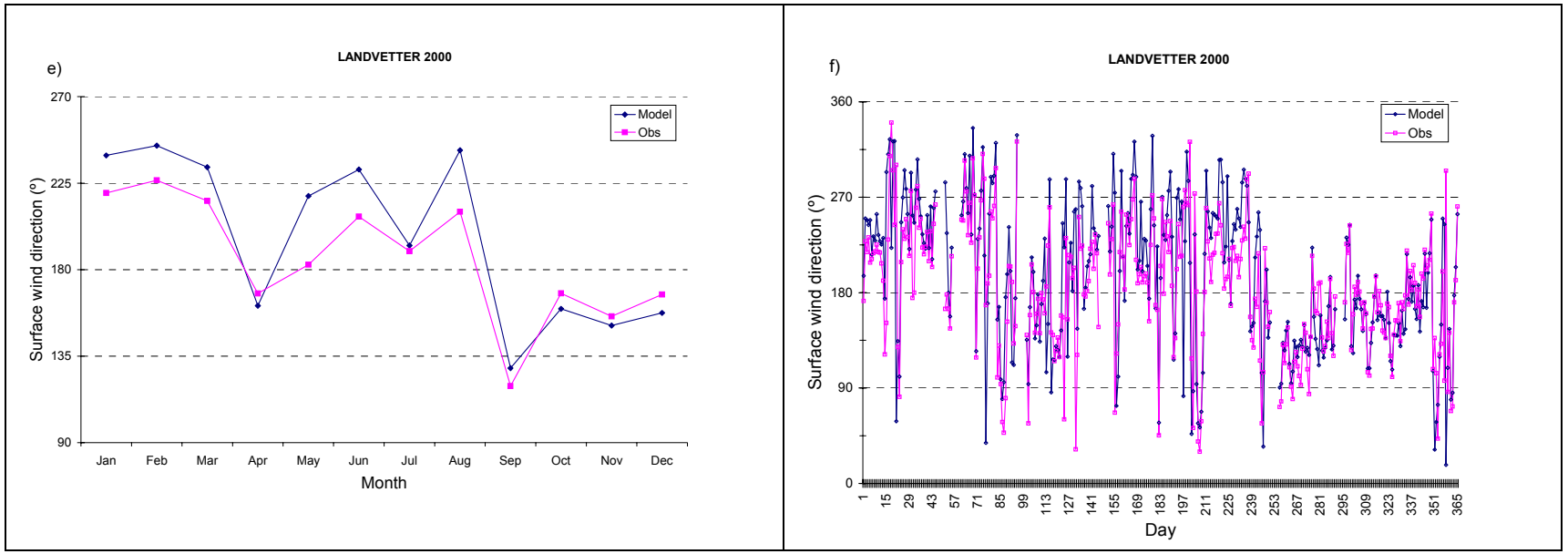

Figure 9. The observed and modeled surface wind direction at Landvetter for 1999 and for 2000 respectively (a, d) diurnal variation; (b, e) seasonal variation; (c, f) daily average.

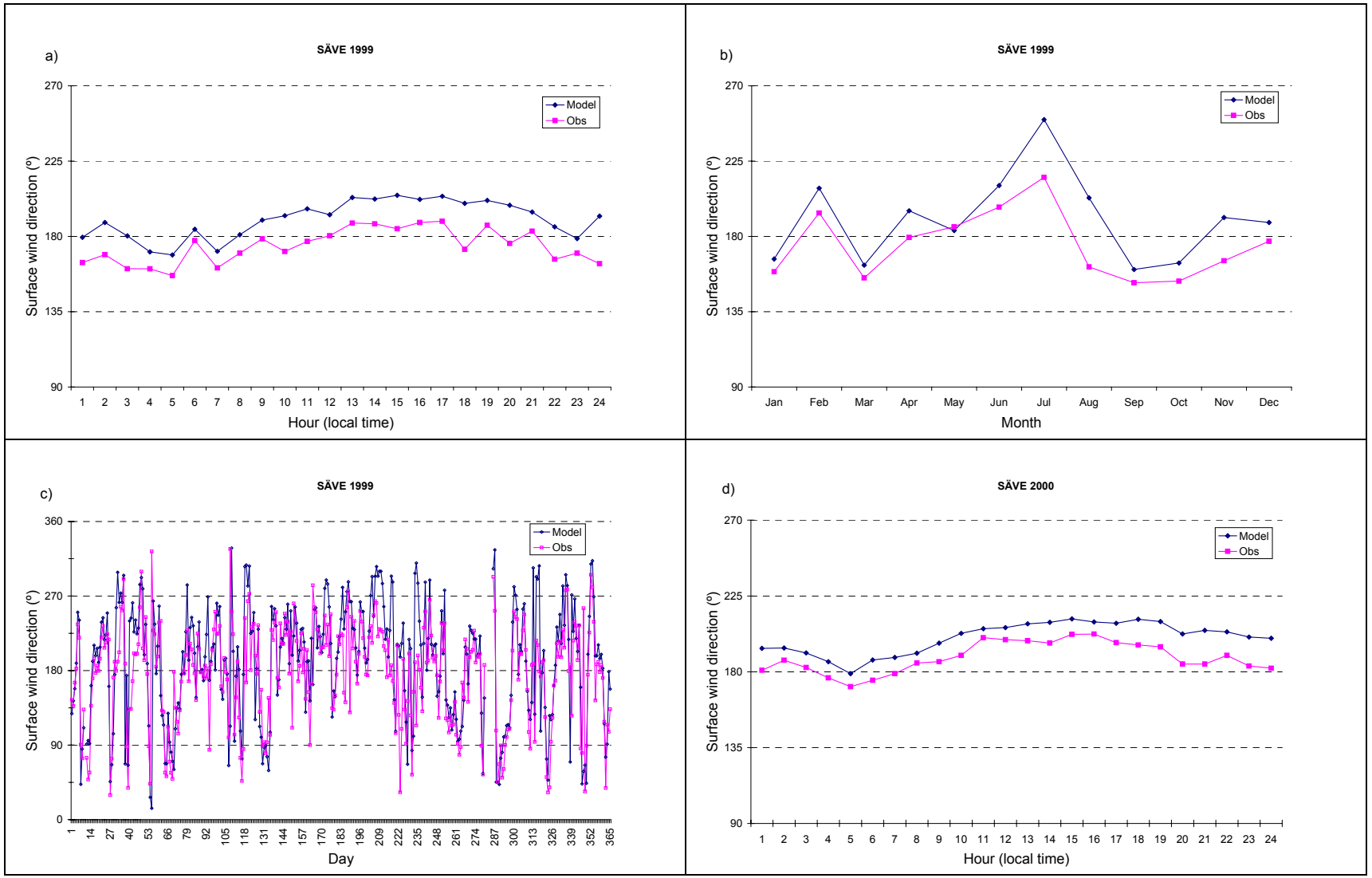
a)
SÄVE 1999
Surface wind direction (°)
270
225
180
135
90
1 2 3 4 5 6 7 8 9 10 11 12 13 14 15 16 17 18 19 20 21 22 23 24
Hour (local time)
Model
Obs
b)
SÄVE 1999
Surface wind direction (°)
270
225
180
135
90
Jan Feb Mar Apr May Jun Jul Aug Sep Oct Nov Dec
Month
Model
Obs
c)
SÄVE 1999
Surface wind direction (°)
360
270
180
90
0
1 14 27 40 53 66 79 92 105 118 131 144 157 170 183 196 209 222 235 248 261 274 287 300 313 326 339 352 365
Day
Model
Obs
d)
SÄVE 2000
Surface wind direction (°)
270
225
180
135
90
1 2 3 4 5 6 7 8 9 10 11 12 13 14 15 16 17 18 19 20 21 22 23 24
Hour (local time)
Model
Obs

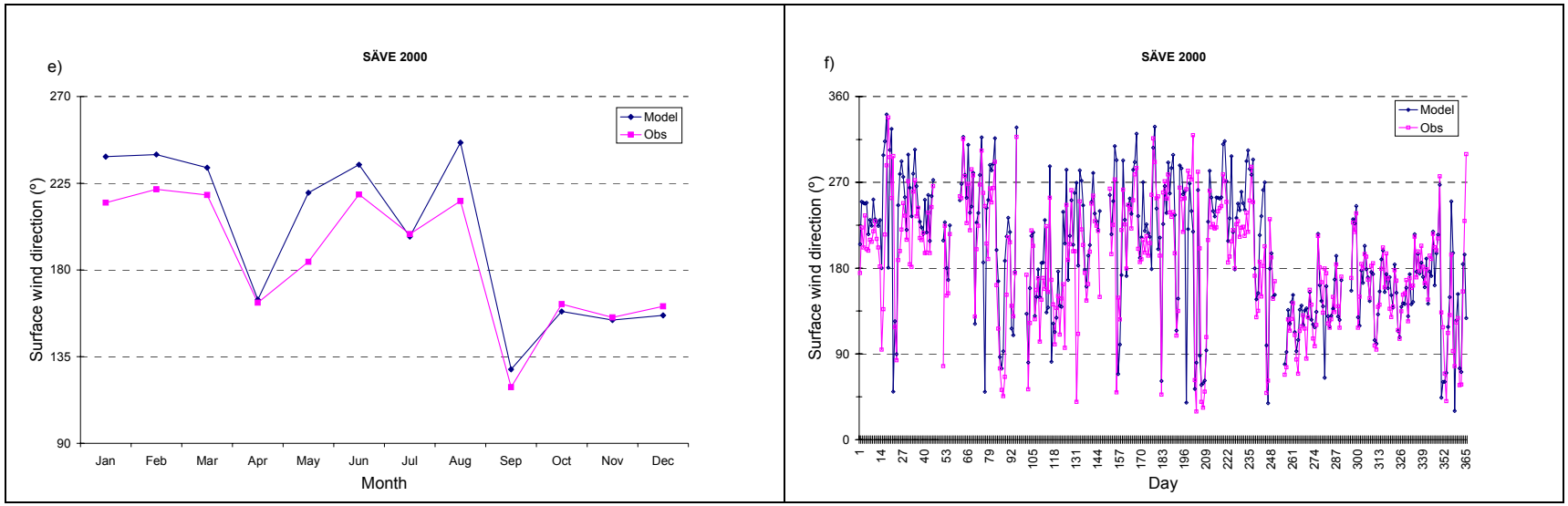

Figure 10. The observed and modeled surface wind direction at Säve for 1999 and for 2000 respectively (a, d) diurnal variation; (b, e) seasonal variation; (c, f) daily average.

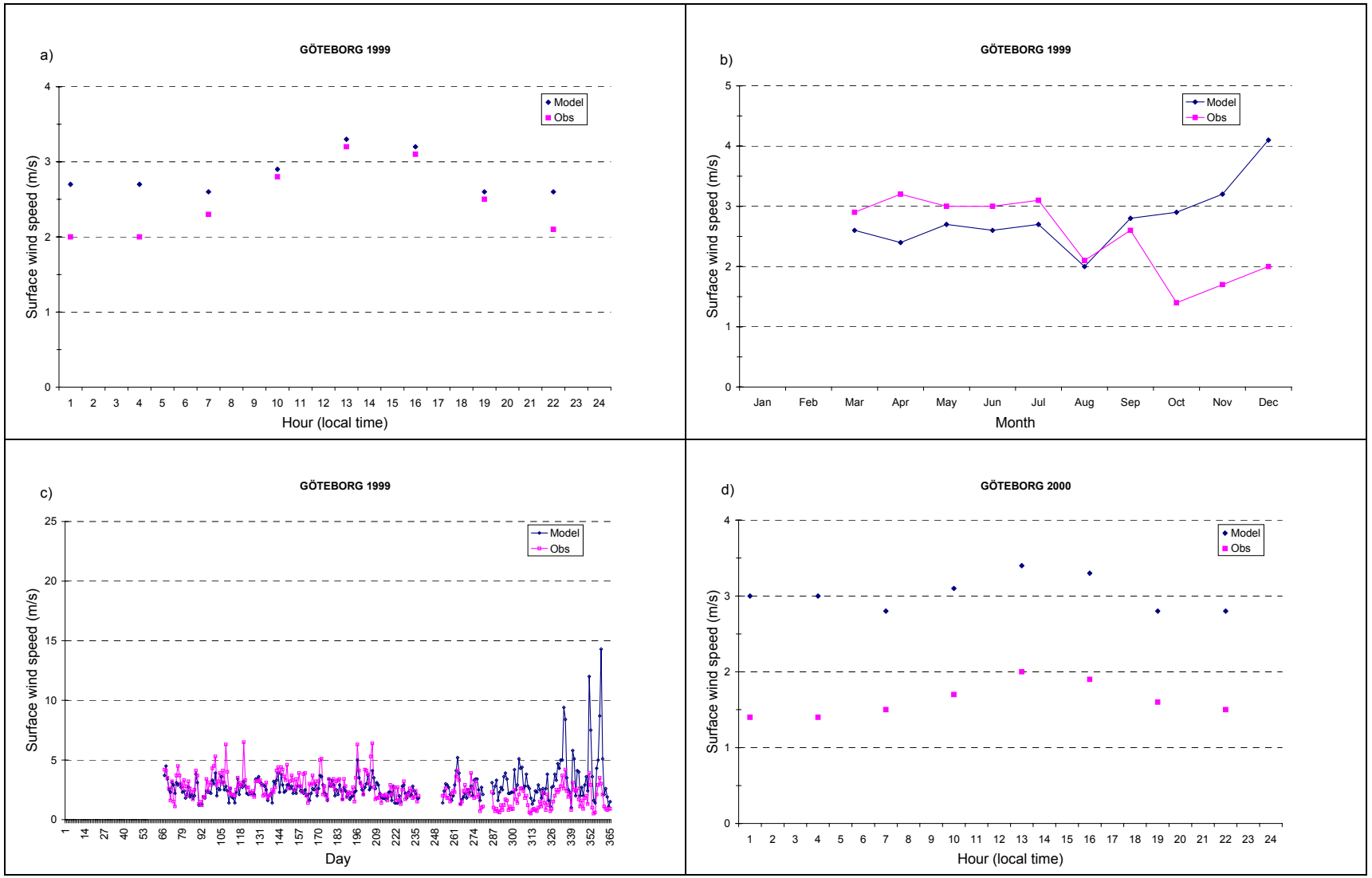
a)
GÖTEBORG 1999
Model
Obs
Surface wind speed (m/s)
Hour (local time)
b)
GÖTEBORG 1999
Model
Obs
Surface wind speed (m/s)
Jan
Feb
Mar
Apr
May
Jun
Jul
Aug
Sep
Oct
Nov
Dec
Month
c)
GÖTEBORG 1999
Model
Obs
Surface wind speed (m/s)
Day
d)
GÖTEBORG 2000
Model
Obs
Surface wind speed (m/s)
Hour (local time)

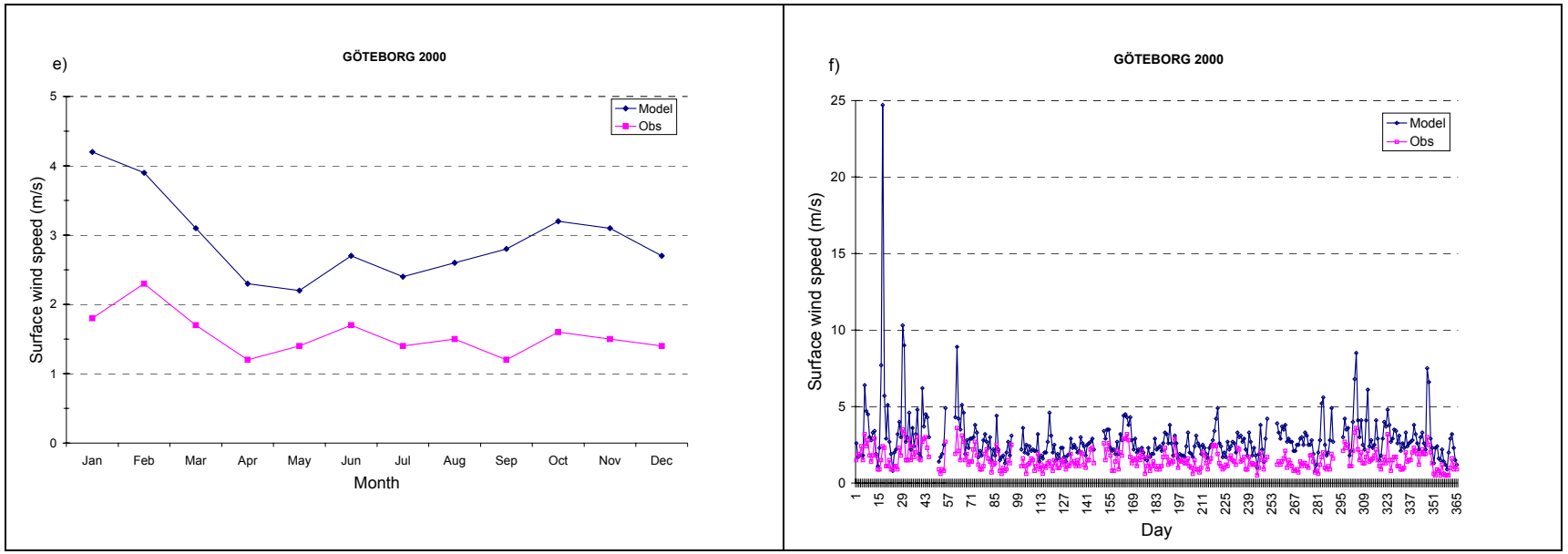

Figure 11. The observed and modeled surface wind speed at Göteborg for 1999 and for 2000 respectively (a, d) diurnal variation; (b, e) seasonal variation; (c, f) daily average.

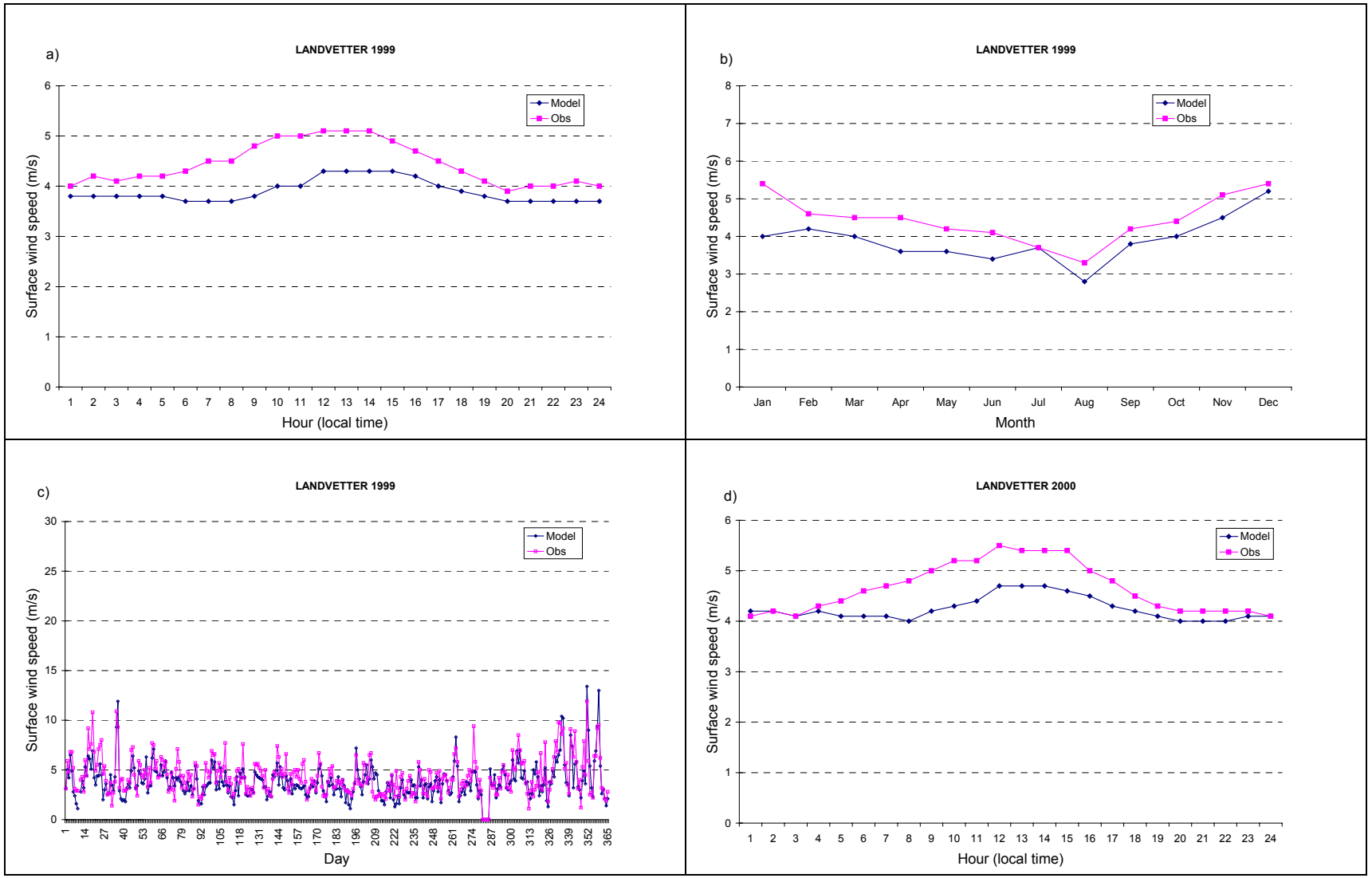
a)
LANDVETTER 1999
Model
Obs
Surface wind speed (m/s)
Hour (local time)
b)
LANDVETTER 1999
Model
Obs
Surface wind speed (m/s)
Jan
Feb
Mar
Apr
May
Jun
Jul
Aug
Sep
Oct
Nov
Dec
Month
c)
LANDVETTER 1999
Model
Obs
Surface wind speed (m/s)
Day
d)
LANDVETTER 2000
Model
Obs
Surface wind speed (m/s)
Hour (local time)

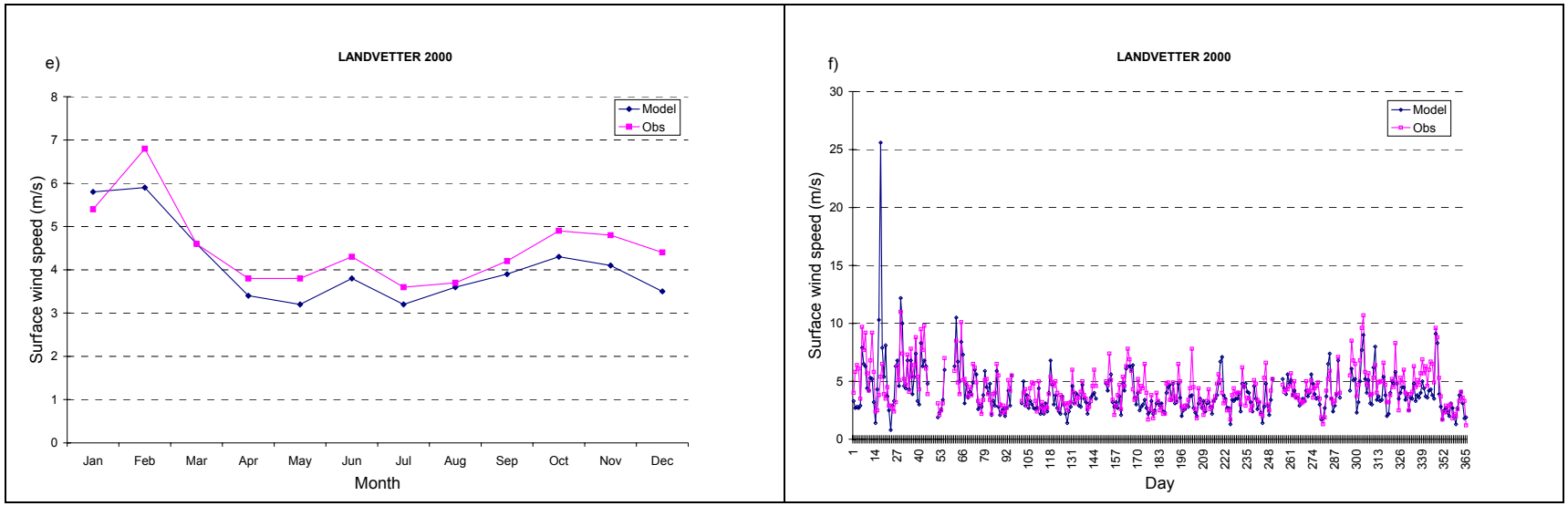

Figure 12. The observed and modeled surface wind speed at Landvetter for 1999 and for 2000 respectively (a, d) diurnal variation; (b, e) seasonal variation; (c, f) daily average.

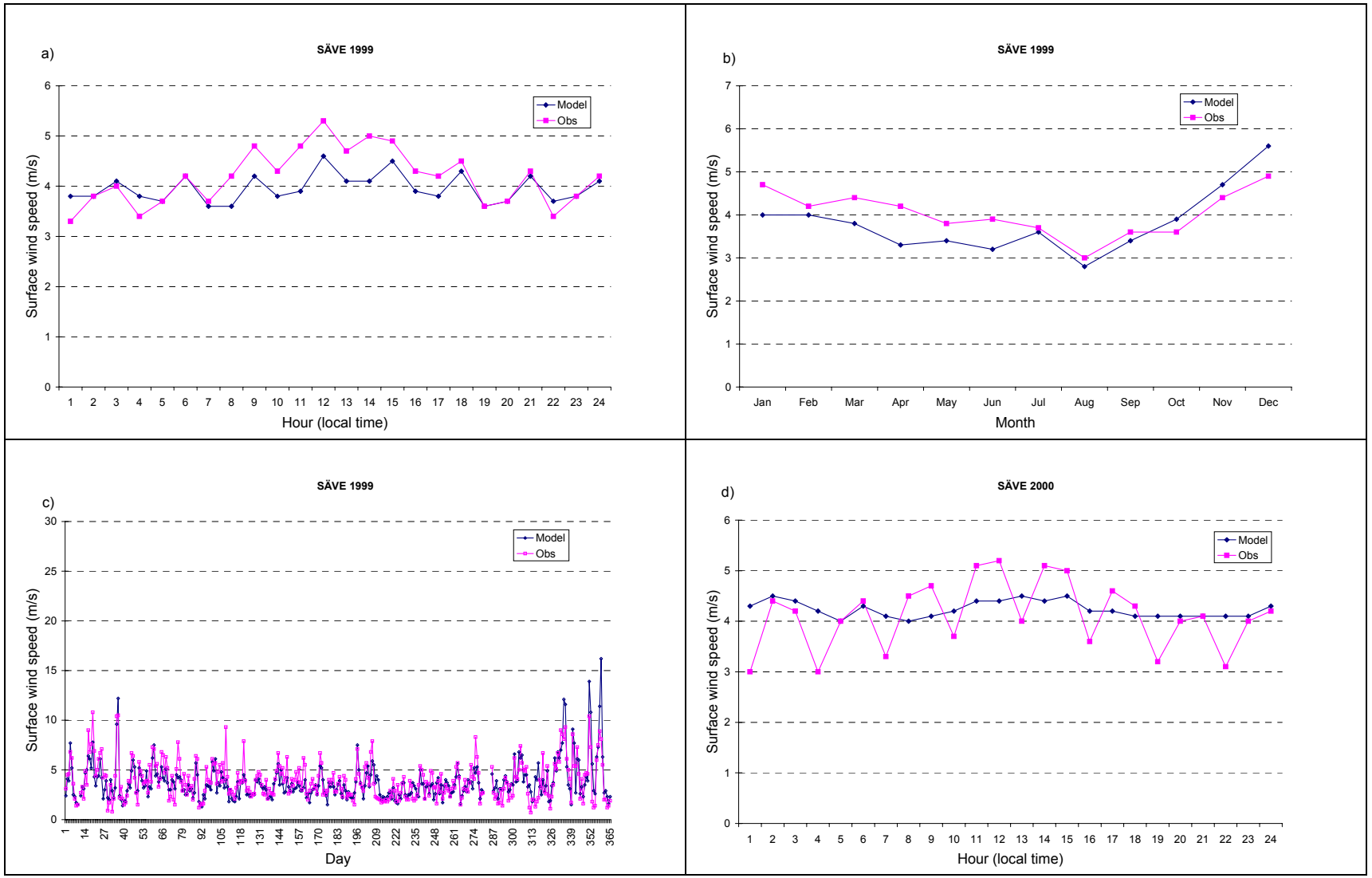
a)
SÄVE 1999
Surface wind speed (m/s)
Hour (local time)
Model
Obs
b)
SÄVE 1999
Surface wind speed (m/s)
Month
Jan
Feb
Mar
Apr
May
Jun
Jul
Aug
Sep
Oct
Nov
Dec
c)
SÄVE 1999
Surface wind speed (m/s)
Day
d)
SÄVE 2000
Surface wind speed (m/s)
Hour (local time)

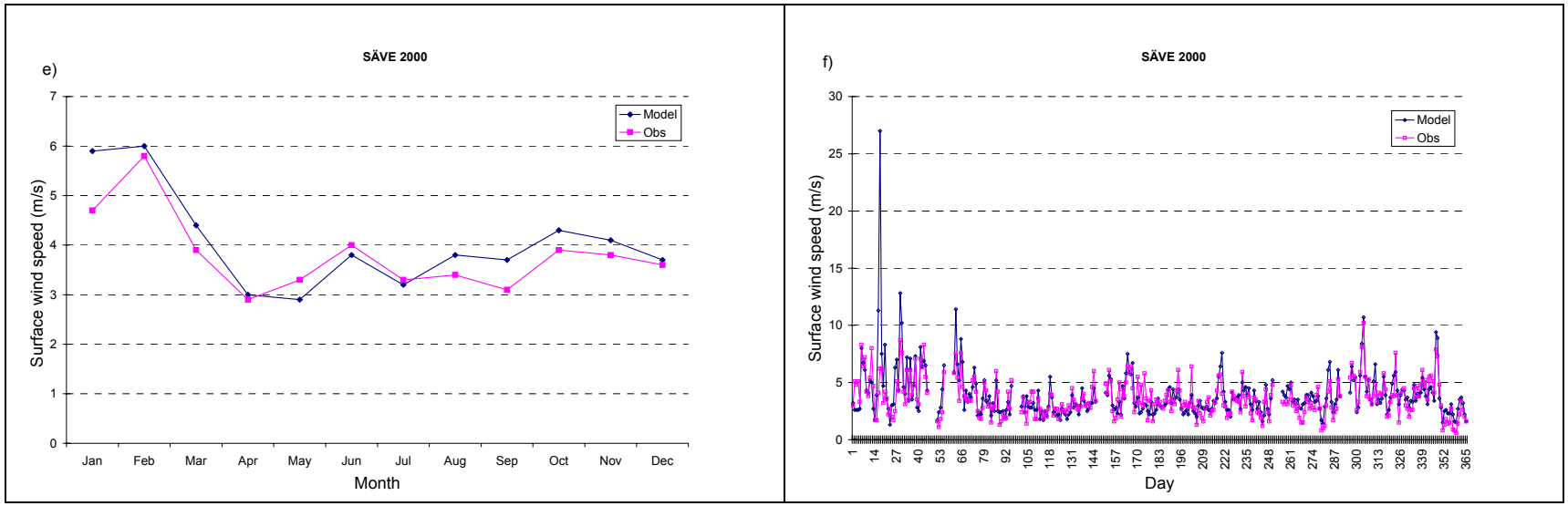

Figure 13. The observed and modeled surface wind speed at Säve for 1999 and for 2000 respectively (a, d) diurnal variation; (b, e) seasonal variation; (c, f) daily average.

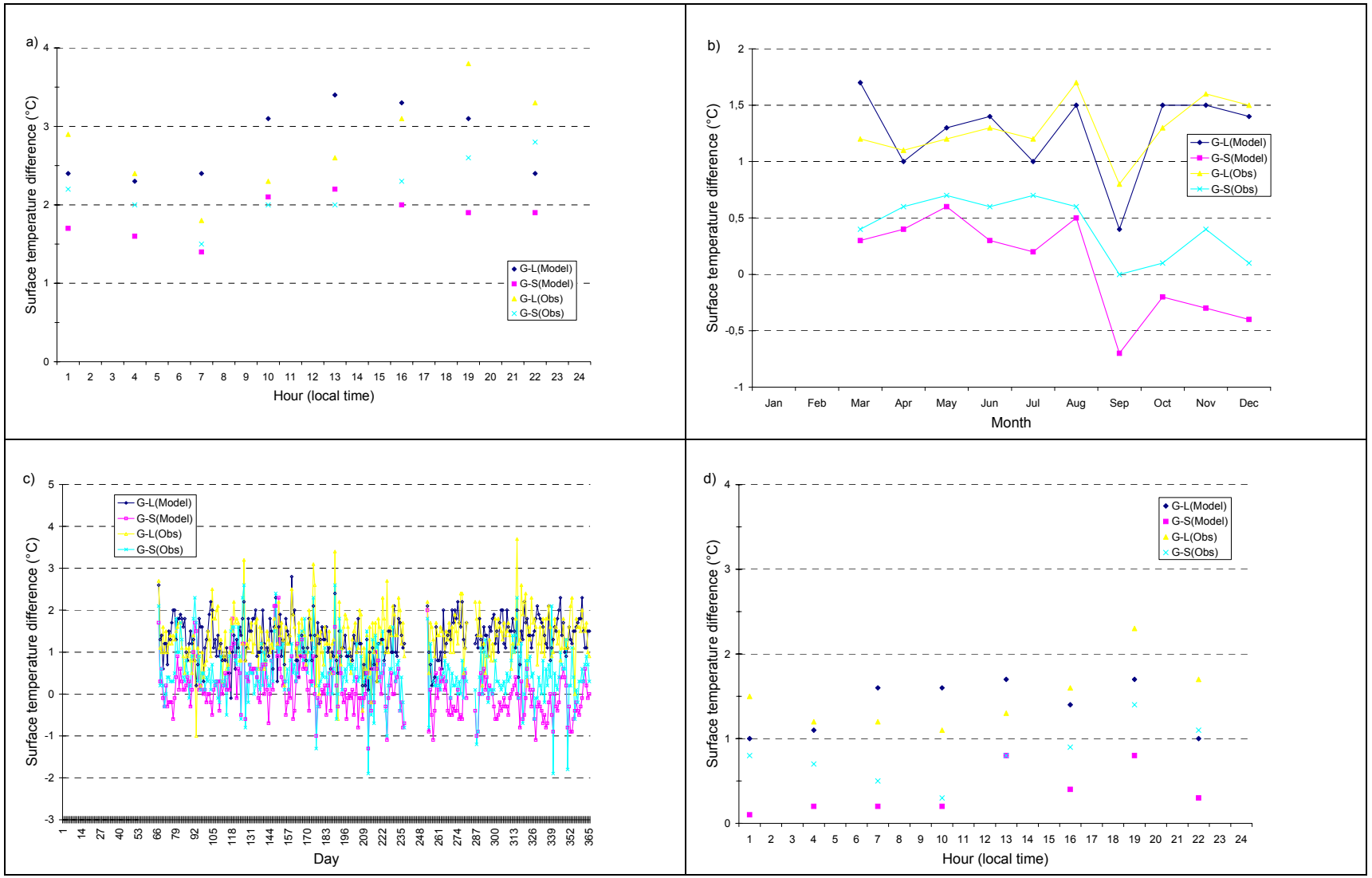
a)
Surface temperature difference (°C)
Hour (local time)
G-L(Model)
G-S(Model)
G-L(Obs)
G-S(Obs)
b)
Surface temperature difference (°C)
Month
Jan
Feb
Mar
Apr
May
Jun
Jul
Aug
Sep
Oct
Nov
Dec
G-L(Model)
G-S(Model)
G-L(Obs)
G-S(Obs)
c)
Surface temperature difference (°C)
Day
G-L(Model)
G-S(Model)
G-L(Obs)
G-S(Obs)
d)
Surface temperature difference (°C)
Hour (local time)
G-L(Model)
G-S(Model)
G-L(Obs)
G-S(Obs)

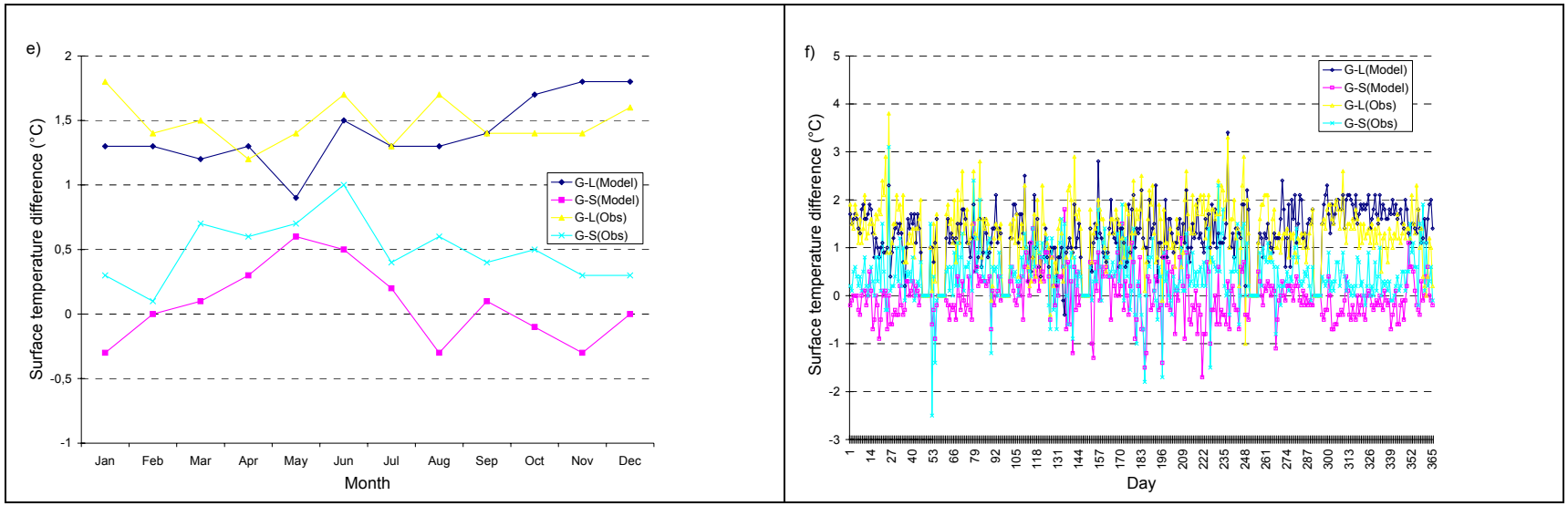

Figure 14. The observed and modeled surface temperature between Göteborg and Landvetter (G-L), as well as between Göteborg and Säve (G-S) for 1999 and for 2000 respectively (a, d) diurnal variation; (b, e) seasonal variation; (c, f) daily average.

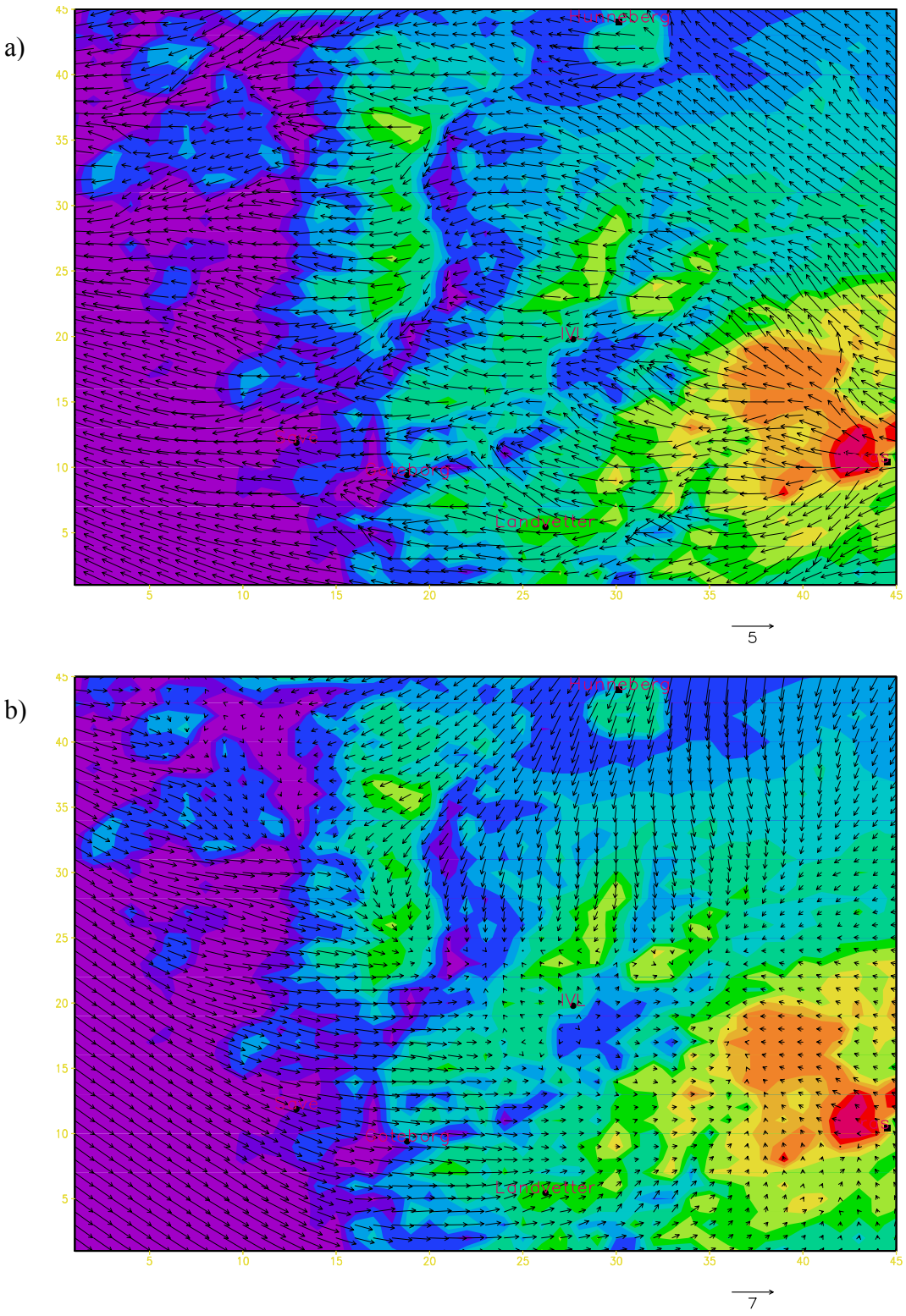

Figure 15. The modeled surface wind during night and day on 12 June 1999 a) at 03:00 local time; b) at 15:00 local time.

a)

b)

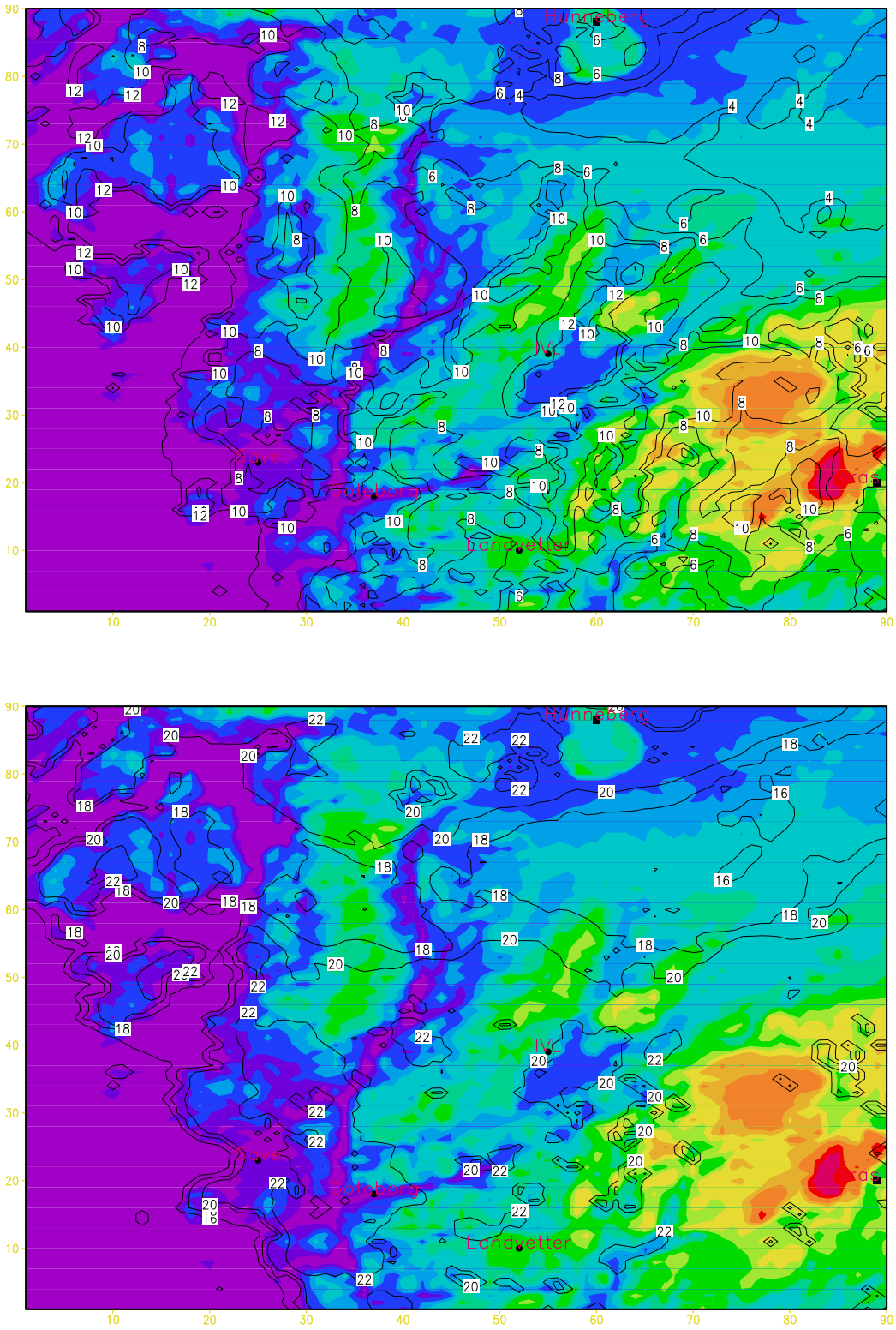

Figure 16. The modeled surface air temperature (^{o}C) during night and day on 12 June 1999 (a) at 03:00 local time; (b) at 15:00 local time.

a)

b)

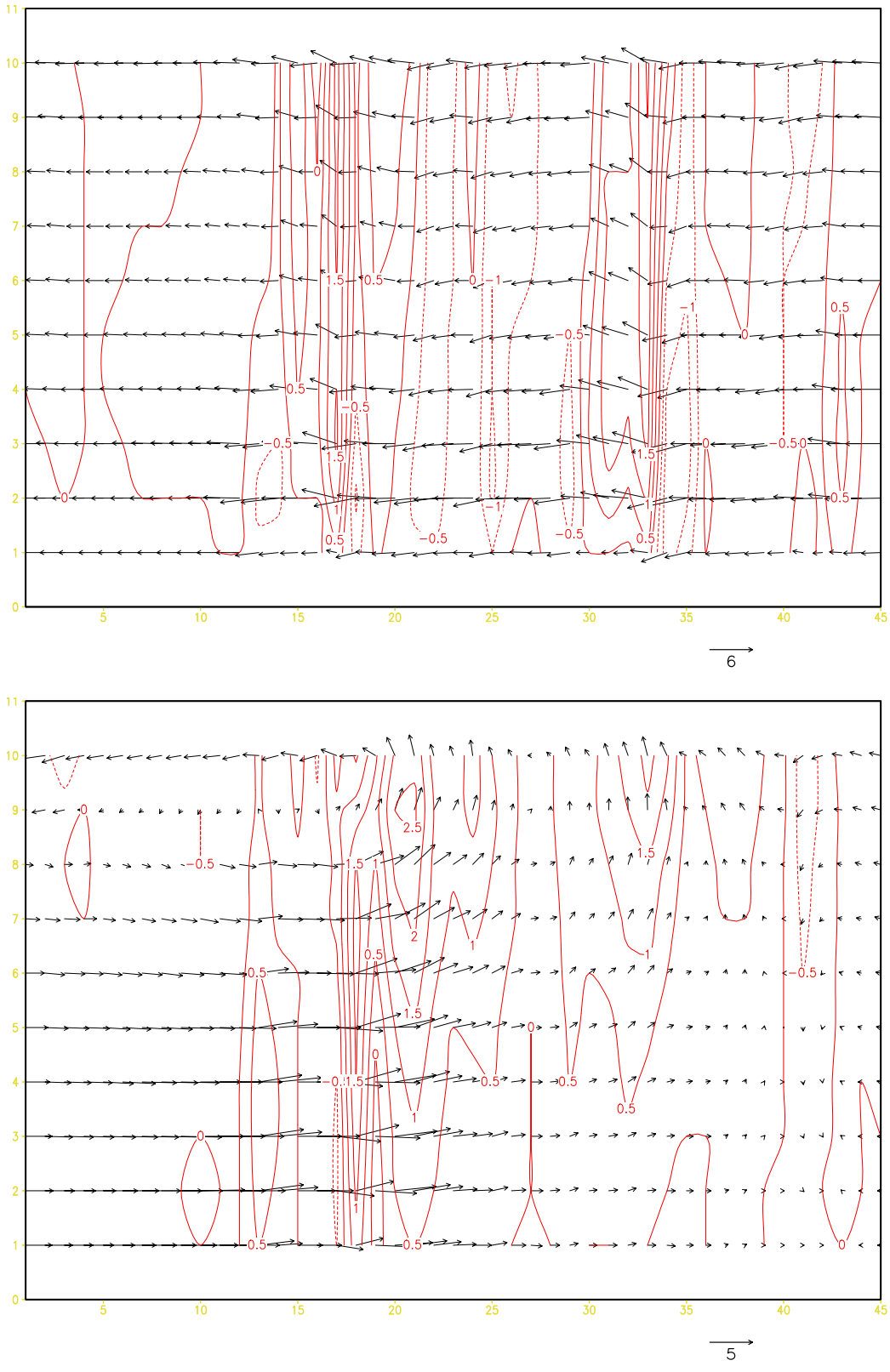

Figure 17. The modeled cross section (X-Z or u-10w) of wind during night and day on 12 June 1999 a) at 03:00 local time; b) at 15:00 local time. Unit of u and w m/s.

a)

b)

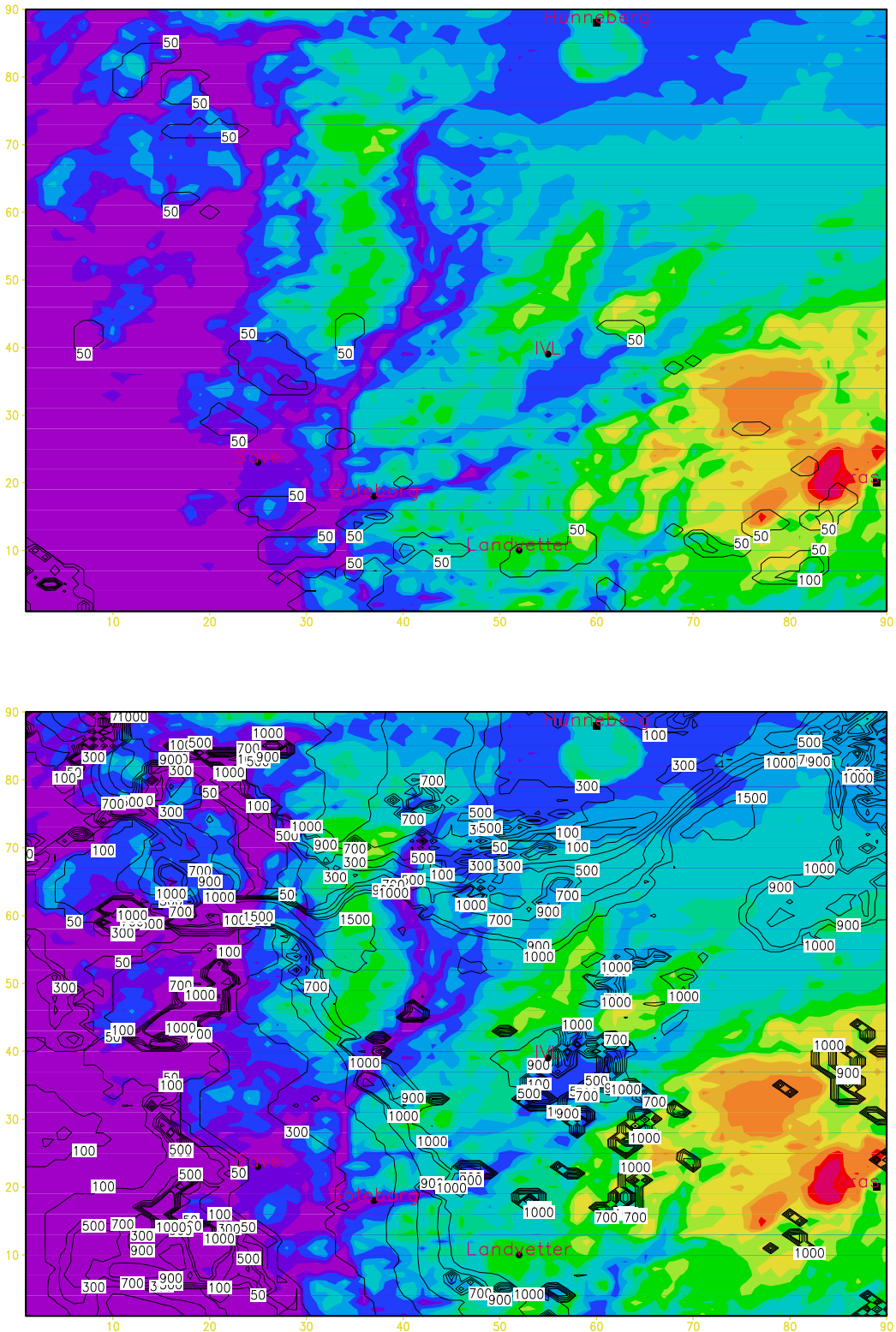

Figure 18. The modeled mixing height (m) during night and day on 12 June 1999 a) at 03:00 local time; b) at 15:00 local time.

Table 3a. Comparison between the modeled and observed wind profiles at Hunneberg in 1999. Unit of wind speed: m/s.

Component	*Height*	*Correlation coefficient*	*Modeled average*	*Observed average*	*Bias*	*RMSE*
wind-u	**50m** (7672*)	0.78				0.2
wind-v		0.66				0.2
wind speed		0.54	6.0	3.5	2.5	0.2
wind-u	**100m** (7674*)	0.81				0.2
wind-v		0.70				0.2
wind speed		0.60	7.0	5.5	1.5	0.3
wind-u	**150m** (7658*)	0.82				0.2
wind-v		0.70				0.2
wind speed		0.62	7.8	6.6	1.2	0.3
wind-u	**200m** (7015*)	0.81				0.2
wind-v		0.70				0.2
wind speed		0.57	8.5	7.2	1.3	0.3
wind-u	**300m** (3908*)	0.76				0.3
wind-v		0.69				0.3
wind speed		0.50	9.5	7.8	1.7	0.4
wind-u	**400m** (1253*)	0.73				0.4
wind-v		0.68				0.4
wind speed		0.51	10.5	8.2	2.3	0.5

* sample number for statistics

Table 3b. Comparison between the modeled and observed wind profiles at Hunneberg in 2000. Unit of wind speed: m/s.

Component	*Height*	*Correlation coefficient*	*Modeled average*	*Observed average*	*Bias*	*RMSE*
wind-u	**50m** (100*)	-0.46				0.9
wind-v		0.57				0.6
wind speed		0.39	5.4	4.1	1.3	0.9
wind-u	**100m** (5603*)	0.65				0.3
wind-v		0.42				0.3
wind speed		0.47	8.2	4.7	3.5	0.3
wind-u	**150m** (5601*)	0.64				0.3
wind-v		0.44				0.3
wind speed		0.51	9.0	6.5	2.5	0.3
wind-u	**200m** (5571*)	0.62				0.3
wind-v		0.48				0.3
wind speed		0.50	9.7	7.4	2.3	0.4
wind-u	**300m** (4681*)	0.53				0.3
wind-v		0.52				0.3
wind speed		0.45	10.6	8.2	2.4	0.4
wind-u	**400m** (2923*)	0.37				0.4
wind-v		0.45				0.4
wind speed		0.22	11.2	8.4	2.8	0.5

* sample number for statistics

Table 4a. Comparison between the modeled and observed wind profiles at Borås in 1999. Unit of wind speed: m/s.

Component	*Height*	*Correlation coefficient*	*Modeled average*	*Observed average*	*Bias*	*RMSE*
Wind-u	**50m** (7297*)	0.80				0.2
Wind-v		0.71				0.2
Wind speed		0.60	5.3	3.8	1.5	0.2
Wind-u	**100m** (7851)	0.83				0.2
Wind-v		0.72				0.2
Wind speed		0.64	6.6	5.0	1.6	0.2
wind-u	**150m** (7364*)	0.77				0.2
wind-v		0.71				0.2
wind speed		0.49	7.5	5.5	2.0	0.3
wind-u	**200m** (5013*)	0.77				0.3
wind-v		0.71				0.2
wind speed		0.51	8.0	6.1	1.9	0.3
wind-u	**300m** (1544*)	0.81				0.4
wind-v		0.67				0.4
wind speed		0.45	9.8	8.0	1.8	0.4
wind-u	**400m** (298*)	0.87				0.5
wind-v		0.70				0.5
wind speed		0.56	11.7	9.6	2.1	0.6

* sample number for statistics

Table 4b. Comparison between the modeled and observed wind profiles at Borås in 2000. Unit of wind speed: m/s.

Component	*Height*	*Correlation coefficient*	*Modeled average*	*Observed average*	*Bias*	*RMSE*
wind-u	**50m** (4773*)	-0.07				0.2
wind-v		-0.06				0.2
wind speed		0.01	6.2	2.5	3.7	0.3
wind-u	**100m** (7113*)	0.69				0.2
wind-v		0.53				0.2
Wind speed		0.47	7.7	4.2	3.5	0.3
wind-u	**150m** (7020*)	0.67				0.2
wind-v		0.57				0.3
Wind speed		0.46	8.7	5.5	3.2	0.3
wind-u	**200m** (5013*)	0.77				0.3
wind-v		0.71				0.2
Wind speed		0.51	8.0	6.1	1.9	0.3
wind-u	**300m** (1797*)	0.49				0.4
wind-v		0.57				0.4
Wind speed		0.29	10.7	7.7	3.0	0.5
wind-u	**400m** (404*)	0.30				0.7
wind-v		0.61				0.6
Wind speed		0.12	11.4	9.0	2.4	0.8

* sample number for statistics

5. Model outputs

The output of TAPM is rich, covering 2D fields, such as total solar radiation, net radiation, sensible heat flux, evaporative heat flux, friction velocity, potential virtual temperature, potential temperature, convective velocity, mixing height, screen-level temperature, screen-level relative humidity, surface temperature, rainfall, as well as 3D fields, such as horizontal wind speed, horizontal wind direction, vertical velocity, temperature , relative humidity, potential temperature, turbulence kinetic energy.

As examples, Figure 18 gives a snapshot of modeled mixing height during a day and a night. The figure shows distinct diurnal variation of mixing height, which is strong at the day time due to the unstable atmsophere and weak at the nightime due to the stable stratification of the atmosphere.

6. Comments on use of TAPM

6.1.Computer requirements

TAPM takes a long time to run and requires a fast PC. Run-time will vary depending on your choice of model options.

6.2 Model limitations

Although TAPM performs well in many aspects, it has some major limitations as following:

(1) TAPM should not be used for larger domains than 1000 km by 1000 km.

(2) The GRS photochemistry option in the model may not be suitable for examining small perturbations in emissions inventories, particularly in VOC emissions, due to the highly lumped approach taken for VOCs in this mechanism. VOC reactivities should also be chosen carefully for each region of application.

6.3. Soil moisture setting

The soil moisture is an import parameter in determining the surface energy balance. Based on our experience, it should be set variable with season. As such, the following soil moisture is recommended for the model running, which are listed in Table 5.

Table 5. Deep soil volumetric moisture used in model run

Mon	*Jan*	*Feb*	*Mar*	*Apr*	*May*	*Jun*	*Jul*	*Aug*	*Sep*	*Oct*	*Nov*	*Dec*
Value	0.29	0.30	0.28	0.24	0.21	0.19	0.18	0.19	0.21	0.23	0.26	0.28

6.4. Output processing

Two extra programs (tapm2outa.exe and glc2glca.exe) can be used to transform the TAPM binary outputs into ASCII format, which can be seen in Appendix in detail.

Another two programs, named readmet.exe and readcon.exe, have been designed to convert ASCII format files into binary format for Grads uses, also see Appendix.

The output of TAPM can also be presented based on Grads system using *.gs files.

7. Conclusions

Based on the comparisons between the TAPM output from the two years run and the surface/profile measurements on air temperature and wind, it has been found that TAPM performs well in simulating air temperature and wind, which are the two most important fields to drive the air pollution modelling. In addition, TAPM has strong ability in modelling sea-land breeze and urban heat island effect. As such, it is concluded that TAPM can be applied in meteorological modelling and environmental impact assessment in Sweden with some confidence in the future.

Reference

Hurley, P.J. (1999a). 'The Air Pollution Model (TAPM) Version 1: Technical Description and Examples', *CAR Technical Paper No. 43*. 42 p.

Hurley, P.J. (1999b). 'The air pollution model (TAPM) version 1: User manual'. Internal paper 12 of CSIRO Atmospheric Research Division 22 p.

Appendix Tools developed

1. tapm2outa.exe

It converts TAPM meteorological output *.out and *.rfl files to an ASCII *.outa file. For all or a subset of specified dates can be run using the following command:

echo sdate edate t100a | tapm2outa.exe

where, sdate is the start date (yyyymmdd) that you want in the *.outa file,

edate is the end date (yyyymmdd) that you want in the *.outa file,

t100a is the filename prefix for the *.out file (e.g. t100a.out) and produces a *.outa file (e.g. t100a.outa). The file format for the *.outa file is as follows :

- fixed format with READ1 using format 10i8 (10 integers per line with each integer using 8 characters)
- fixed format with READ2 using format 10f8.2 (10 floating point numbers per line with each number using 8 characters with 2 digits after the decimal point)

READ1: nx, ny, nz, dx, dy

READ2: ((zs(i,j),i=1,nx),j=1,ny)

READ2: (((z(i,j,k),i=1,nx),j=1,ny),k=1,nz)

Repeated for each simulation hour:

READ1: date, hour

READ2: ((tsr(i,j),i=1,nx),j=1,ny)

READ2: ((net(i,j),i=1,nx),j=1,ny)

READ2: ((sens(i,j),i=1,nx),j=1,ny)

READ2: ((evap(i,j),i=1,nx),j=1,ny)

READ2: ((ustar(i,j),i=1,nx),j=1,ny)

READ2: ((pvstar(i,j),i=1,nx),j=1,ny)

READ2: ((ptstar(i,j),i=1,nx),j=1,ny)

READ2: ((wstar(i,j),i=1,nx),j=1,ny)

READ2: ((zmix(i,j),i=1,nx),j=1,ny)

READ2: ((tscr(i,j),i=1,nx),j=1,ny)

READ2: ((rhscr(i,j),i=1,nx),j=1,ny)

READ2: ((tsurf(i,j),i=1,nx),j=1,ny)

READ2: ((rain(i,j),i=1,nx),j=1,ny)

READ2: (((ws(i,j),i=1,nx),j=1,ny),k=1,nz)

READ2: (((wd(i,j),i=1,nx),j=1,ny),k=1,nz)

READ2: (((ww(i,j),i=1,nx),j=1,ny),k=1,nz)

READ2: (((tt(i,j),i=1,nx),j=1,ny),k=1,nz)

READ2: (((rh(i,j),i=1,nx),j=1,ny),k=1,nz)

READ2: (((pt(i,j),i=1,nx),j=1,ny),k=1,nz)

READ2: (((tke(i,j),i=1,nx),j=1,ny),k=1,nz)

with variables:

nx number of west-east (x) grid points for the meteorological grid,

ny number of south-north (y) grid points for the meteorological grid,

nz number of vertical (z) grid points (levels) for the meteorological grid,

dx west-east (x) grid spacing (m) for the meteorological grid,

dy south-north (y) grid spacing (m) for the meteorological grid,

zs smoothed terrain height (m),

z height above the terrain (m),

date date (yyyymmdd),

hour hour of simulation (1-24),

tsr total solar radiation (W m-2),

net net radiation (W m-2),

sens sensible heat flux (W m-2),

evap evaporative heat flux (W m-2),

ustar friction velocity scale (m s-1),

pvstar potential virtual temperature scale (K),

ptstar potential temperature scale (K),

wstar convective velocity scale (m s-1),

zmix mixing height (m),

tscr screen-level temperature (K),

rhsrc screen-level relative humidity (%),

tsurf surface temperature (K),

rain rainfall (mm hr-1),

ws horizontal wind speed (m s-1),

wd horizontal wind direction (o) (usual meteorological definition),

ww vertical velocity (m s-1),

tt temperature (K),

rh relative humidity (%),

pt potential temperature (K),

tke turbulence kinetic energy (m2 s-2).

Note that the meteorological grid (array) is oriented so that:

grid(1, 1, 1) is the south-west corner at the surface,

grid(nx, 1, 1) is the south-east corner at the surface,

grid(1,ny, 1) is the north-west corner at the surface,

grid(nx,ny, 1) is the north-east corner at the surface,

and similarly for array index k = nz at the top of the grid.

2. glc2glca.exe

It converts a TAPM concentration output *.glc file to an ASCII *.glca file and can be run using the following command:

echo t100atr1 | glc2glca.exe

where,

t100atr1 is the filename prefix for the *.glc file (e.g. t100atr1.glc) and produces a *.glca file (e.g. t100atr1.glca).The file format for *.glca files is as follows (space delimited free format):

READ: nx, ny

Repeated for each simulation hour:

READ: idate, itime

READ: ((ic(i,j),i=1,nx),j=1,ny)

with variables:

nx	number of west-east (x) grid points for the concentration grid,
ny	number of south-north (y) grid points for the concentration grid,
idate	date (yyyymmdd),
itime	hour of simulation,
ic	concentration grid (array).

Note that the array is oriented so that

ic(1, 1) is the south-west corner,

ic(nx, 1) is the south-east corner,

ic(1 ,ny) is the north-west corner,

ic(nx,ny) is the north-east corner.

3. readmet.exe

It converts TAPM meteorology output ASCII file(such as t10a.outa) to bin format file and can be run using the following command:

echo sdate fname | readmet.exe

where, sdate is starting date(6 characters, yymmdd) and fname is the file name of ASCII file(4 characters, for example, t10a).

4. readcon.exe

It converts TAPM concentration output ASCII file to binary format file and can be run using the following command:

echo fname | readcon.exe

where, fname is the file name of ASCII file(7 characters, for example, t10atr1)

5. *.gs

All *.gs files are used to present the TAPM outputs based on Grads system.